ERS-2 Wind Scatterometer Cyclic Report

from 15th November 1999 to 20th December 1999
Cycle 48

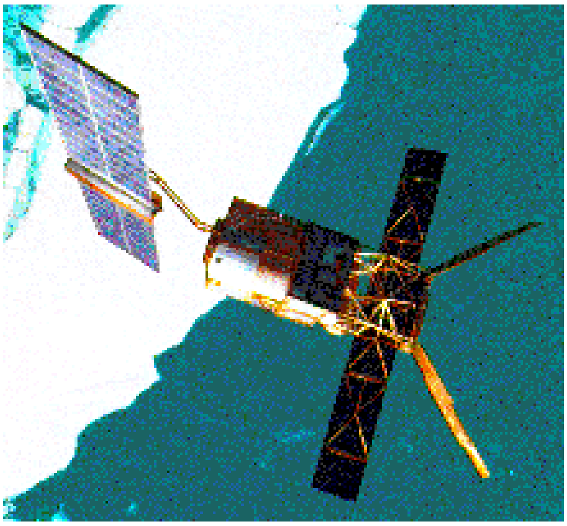

Prepared by:	PCS team	ESRIN APP-ADQ
Inputs from:	F. Aidt L. Isaksen	ESTEC TOS-EMS ECMWF

Document No: APP-ADQ/PCS/WS00-001
Issue: 1.0
Date: 21st, January 2000

Distribution List

ESAHQ	G. Duchossois	
ESTEC	M. Canela	APP-LR
	E. Attema	SCI-VRS
	F. Aidt	TOS-EMS
	B. Gelsthorpe	APP-LTP
	R. Zobl	
	K. van't Klooster	
ESOC	F. Bosquillon de Frescheville	TOS-OFC
	L. Stefanov	TOS-OFC
ESRIN	M. Albani	APP-AD
	P. Lecomte	APP-ADQ
	V. Beruti	APP-ADF
	S. Jutz	APP-ADU
	G. Kohlhammer	APP-AM
	M. Onnestam	APP-ADC
	U.Gebelein	Serco

L.A. Breivik	DNMI
P. Snoeij	DUT
J. Heidbreder	DORNIER
L. Isaksen	ECMWF
J. Kerkman, J. Figa	EUMETSAT
S. Pouliquen	F-PAF
V. Wismann	IFARS
A. Cavanie	IFREMER
R.S. Dunbar	JPL
A. Stoffelen	KNMI
G. Legg, P. Chang	NOAA/NESDIS
W. Gemmill	NOAA/NWS
J. Hawkins	NRL
D. Offiler, R. Graham, C.A. Parrette	UK-MET Office
F. Courtier, H. Roquet	Meteo-France
C. Scupniewicz	FNMOC
R.A. Brown	University of Washington
J. Boutin	LODYC/UPMC

This report and its annex are also available via FTP.
ftp pooh.esrin.esa.it (login as anonymous)
cd pub/SCATTEROMETER
wscatt_rep_48.ps.Z, annex_rep_48.ps.Z

1.0 Introduction and summary

The results reported in each section concern, apart from a summary of the daily quality control made within the PCS, the investigations and the study of “open-problems” related to the scatterometer, e.g. the CMOD-4 for high wind speed, the antenna pattern. In each section results are shown from the beginning of the mission in order to allow comparisons and to outline possible “seasonal” effects. An explanation of the major events that have impacted the performance since launch is given, and a comment about the recent events during the last cycle is included.

This report covers of the period from 15^{th} November 1999 to 20^{th} December 1999 (cycle 48). This report and its annex (the ECMWF reports) are available via ftp (login as anonymous) to the address pooh.esrin.esa.it directory /pub/SCATTEROMETER file names wscatt_rep_48.ps.Z, annex_rep_48.ps.Z (Unix compressed). The report is also available on the PCS web site: http://pcswww.esrin.esa.it (Scatterometer performance page).

The statistics about the availability of the ERS-2 Wind Scatterometer raw data during cycle 48 and the detailed list of the unavailability periods are given in the document “ERS-2 AMI/RA/ATSR/GOME availability statistics” issued at the end of each cycle.

For the calibration performance the results are:

- The evolution of the maximum position of the gamma nought histograms computed over the rain forest is stable. The small decrease in the signal detected during the cycle 48 is within the seasonal fluctuation of the rain forest signal (geophysical effect). For the interbeam calibration the values of the maximum of gamma nought histogram for the aft and fore antenna are very close together. The difference between the fore antenna signal and the mid antenna signal is roughly 0.1 dB (both ascending and descending passes) while the difference between the aft antenna signal and the mid antenna signal seems to have a seasonal behaviour. This difference is close to 0.1 dB during the summer and it is close to 0.2 dB during the winter for the ascending passes. For the descending passes the differences between the winter and the summer is less clear and the aft-mid interbeam calibration is around 0.15 dB (see new plots in section 2.3.3).
- Since the beginning of 1999 the number of valid measurements used to compute the statistics over the rain forest had a clear reduction. In particular for the cycle 48 the gamma nought histograms for the descending passes are available only for the first two weeks. This is due to an increase of SAR images acquired over the Amazon rain forest. The PCS close monitoring this to be sure that the Scatterometer calibration over the rain forest is effectiveness.
- For cycle 48 the antenna patterns over the Brazilian rain forest (large area) are not available from ESTEC due to an hardware problem. The antenna patterns, computed by PCS over a small area of the Brazilian rain forest, for the cycle 48 are very close to the ones obtained in the previous cycle. The antenna patterns show a flat profile, within 0.3 dB for the descending passes and within 0.4dB for the ascending ones.The fore and aft antenna profiles show a small slope in the near-mid range The antenna temperature monitoring over the Brazilian rain forest confirms the increase of roughly 1 degree per year for the mid and fore antenna and roughly 2 degrees per year for the aft antenna. The increase in the antennae temperature could be related with the degradation, during the years, of the antennae protection film.

- The sigma nought biases with respect to the ECMWF model first guess winds are similar to the results from the previous cycle. The antenna patterns show a flat profiles in particular for the near mid range. The biases are slight larger for incident angle above 45 degrees (fore and aft antennae).
- During the cycle 48 the transponders were switched off two times. No new gain constants are available. The description of the antenna pattern is as for the previous report: the antenna patterns are flat but there is a clear shift of the level of the curves. On average, the mid beam is 0.3 dB higher than the aft one and 0.5 dB higher than the fore one. For the descending passes the antenna pattern shows a slight negative slope from far range to near range

For the instrument performance the results of the monitoring are:

- for the internal calibration level the power decrease was 0.06 dB during the cycle 48. The estimation of the power decrease since 26th October 1998 (cycle 37) is, on average, 0.07 dB per cycle. This means that the total power decrease from cycle 37 is 0.84 dB.
- for the Centre of Gravity (CoG) of the received signal an evolution within the nominal range apart from day 8th December 1999 when an orbital manoeuvre caused a change of roughly 100 Hz (50 Hz for the mid beam) in the average CoG for that day.
- for the noise power level a nominal behaviour.

For the product performance the results are:

- The AMI instrument has been operated in scatterometer mode during the ascending passes for 91.4% of the total operation time and during the descending passes for 82.7%; AMI unavailability, descoping and data lost are excluded. Post processed Scatterometer data acquired over tropical cyclones are available from the web site: http://www.pcswww.esrin.esa.it (cyclone tracking page).
- For cycle 48 the PCS quality control has reported stable results apart from a large decrease in the amount of wind measurements due to the payload switch-off on 17th and 18th November 1999 to face out Leonide meteo shower. The wind direction is accurate for the 93% of the nodes, the wind speed bias (UWI-ECMWF forecast) is within 0.5 m/s with a standard deviation of 3.0 m/s.
- The ECMWF reports for the cycle 48 an average wind speed bias of -0.82 m/s (UWI-FG) and -0.58 m/s (FG-4D_Var). The wind speed standard deviation is, on average, 1.5 m/s for FG and 1.6 m/s for the 4D_Var analysis.The wind speed biases are slightly larger than in the previous cycle, and are quite likely due to seasonal variations. The direction standard deviations are ranging between 30 and 65 degrees (UWI-FG) and between 15 and 30 degrees (FG-4D_Var). The directional bias is close to zero for both UWI and 4D_Var analysis. The direction standard deviations are similar to the ones in the previous report period.

2.0 Calibration Performances

The calibration performances are estimated using three types of target: a man made target (the transponder) and two natural targets (the rain forest and the ocean). This approach allow us to design the correct calibration using a punctual but accurate information from transponders and an extended but noisy information from rain forest and ocean for which the main component of the variance comes from the geophysical evolution of the natural target and from the backscattering models used. These aspects are in the calibration performance monitoring philosophy. The major goals of the calibration monitoring activities are the achievement of a “flat” antenna pattern profile and the assurance of a stable absolute calibration level.

2.1 Gain Constant over transponder

One gain constant is computed per transponder per beam from the actual and simulated two-dimensional echo power, which is given as a function of the orbit time and range time. This parameter clearly indicates the difference between “real instrument” and the mathematic model. In order to acquire data over the transponder the Scatterometer must be set into an appropriate operational mode that is defined as “Calibration”.

Table 1 shows the result of the calibration plan for cycle 48. The “Yes” in the EWIC column means that the raw data are available, “No” means the opposite case. The “On” in the transponder status column means that, from the raw data (EWIC), the transponders has been recognised as switched-on; “Off” means the opposite case. The “Yes” in the GC computed column means that a gain constant value has been retrieved, “No” means the opposite case.

During the cycle 48 the transponders were switched off two times (relative orbit 1 and 44). For the relative orbits 237 and 280 transponders data were acquired but results are not yet available.

TABLE 1. Calibration Plan: Cycle 48

DATE	ORBIT (absolute)	ORBIT (relative)	Passage	Ground Station	EWIC (raw data)	AMI mode	Transponder Status	GC computed
991115	23903	1	A	KS	Yes	Calibration	Off	n/a
991118	23946	44	A	MS	Yes	Calibration	Off	n/a
991202	24139	237	D	KS	Yes	Calibration	On	n/a
991205	24182	280	D	KS	Yes	Calibration	On	n/a

Figure 1 and Figure 2 show the gain constants available since the beginning of the mission, the analysis is split for the different antenna elevation angle. From these figure it is clear that the gain constant measurements are stable (within +/-0.5 dB) but after the end of the commissioning phase (cycle 11) only few data are available.

The plots in Figure 3 show the value of the Gain Constant for the three beams and for the ascending, descending and all passes. The plots show the average of all gain constant available since January 1996 (cycle 8) for each antenna elevation angle. The antenna patterns are flat but there is a clear shift of the level of the curves. On average, the mid beam is 0.3 dB higher than the aft one and 0.5 dB higher than the fore one. For the descending passes the antenna pattern shows a slight negative slope from far range to near range.

Since September 1996 ESTEC has added a scaling factor to the gain constant in order to remove the bias among the three antennae. The gain constants were increased by 0.2 dB, -0.3 dB and 0.2 dB, for the fore, mid and aft beam respectively. The result is shown in figure 4. The suggestion given by ESTEC has not been introduced into the ground processing because the antenna patterns computed over the rain forest do not show such bias (see Figure 5). So in the actual scenario, the differences among the antennae are considered as a bias due to the transponder themselves.

ERS-2 Scatterometer Gain Constant History: Ascending Passages

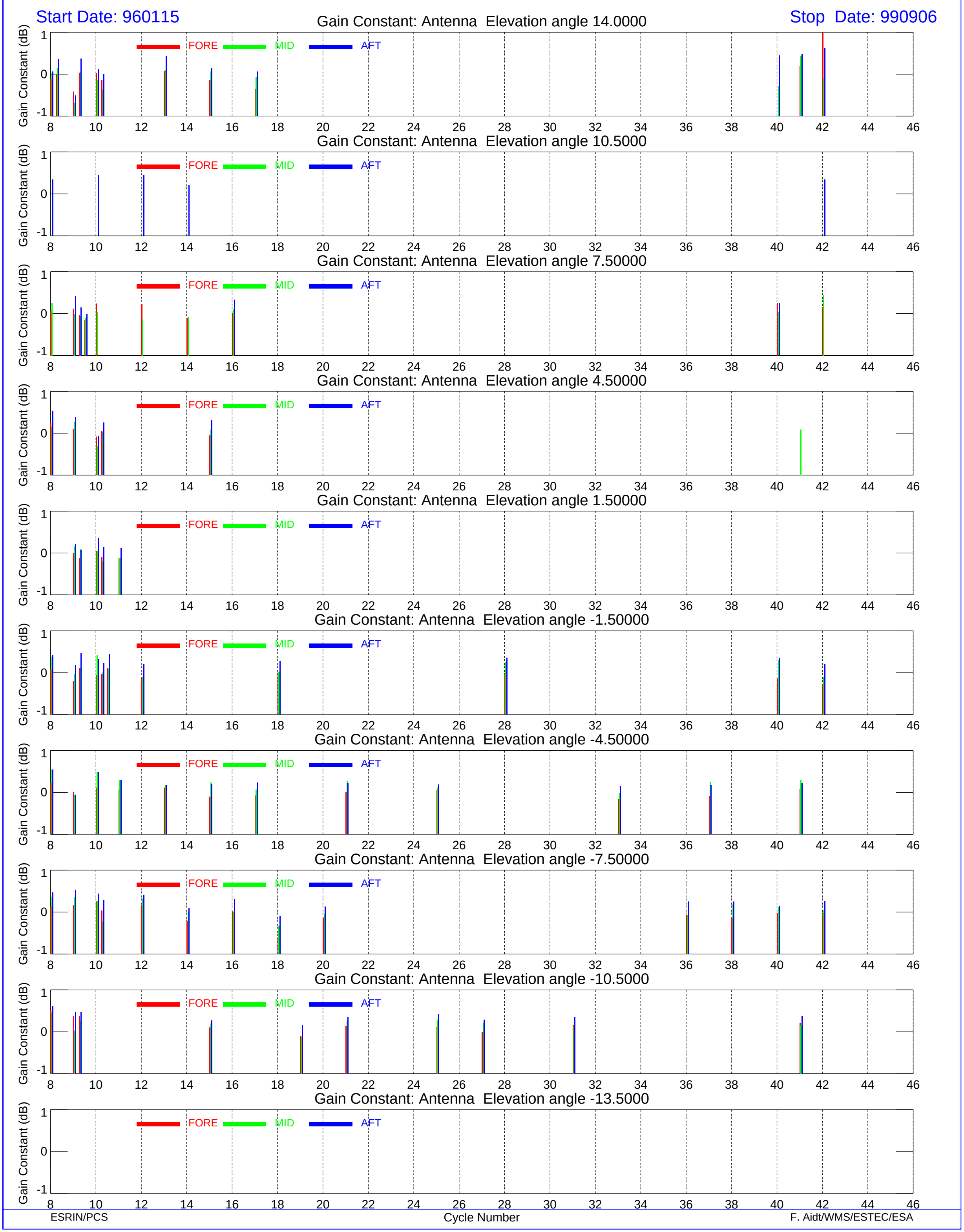

FIGURE 1. ERS-2 Scatterometer; gain Constant over transponder since the beginning of the mission (ascending passes).

ERS-2 Scatterometer Gain Constant History: Descending Passages

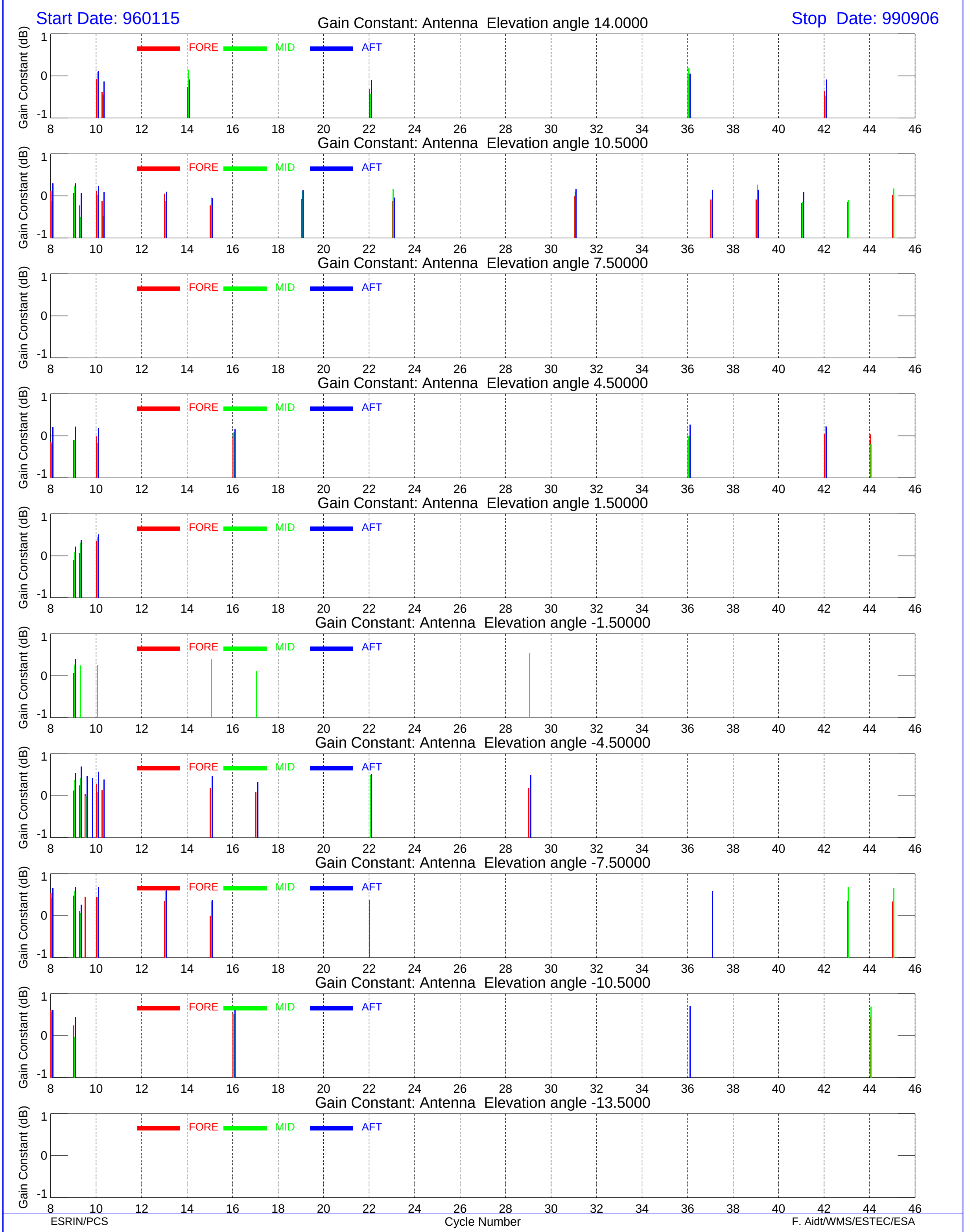

FIGURE 2. Scatterometer; gain Constant over transponder since the beginning of the mission (descending passes)

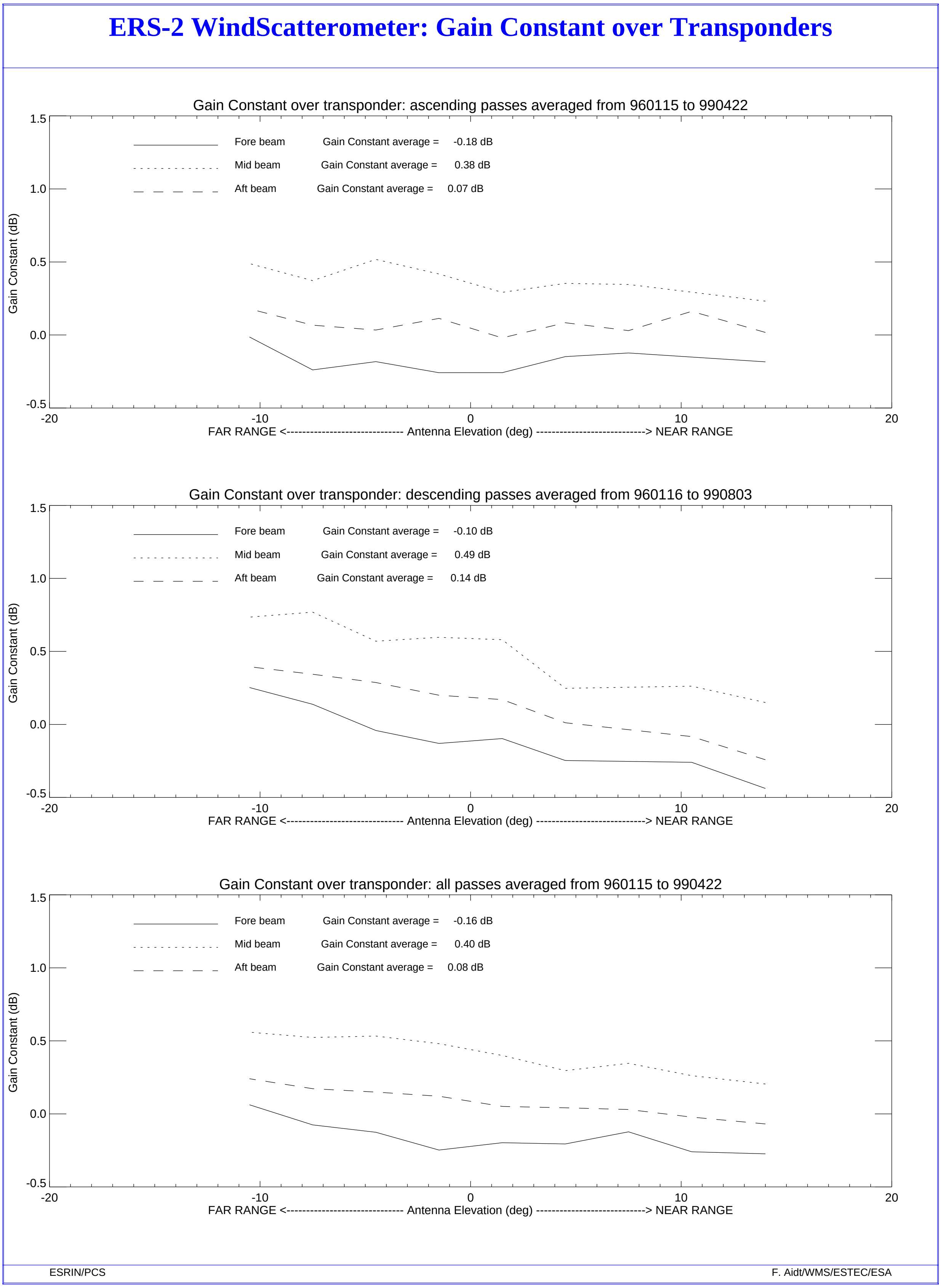

FIGURE 3. ERS-2 Scatterometer: gain constant over transponders. All data available since January 1996. Upper plot: ascending passes. Middle plot: descending passes. Lower plot: all passes.

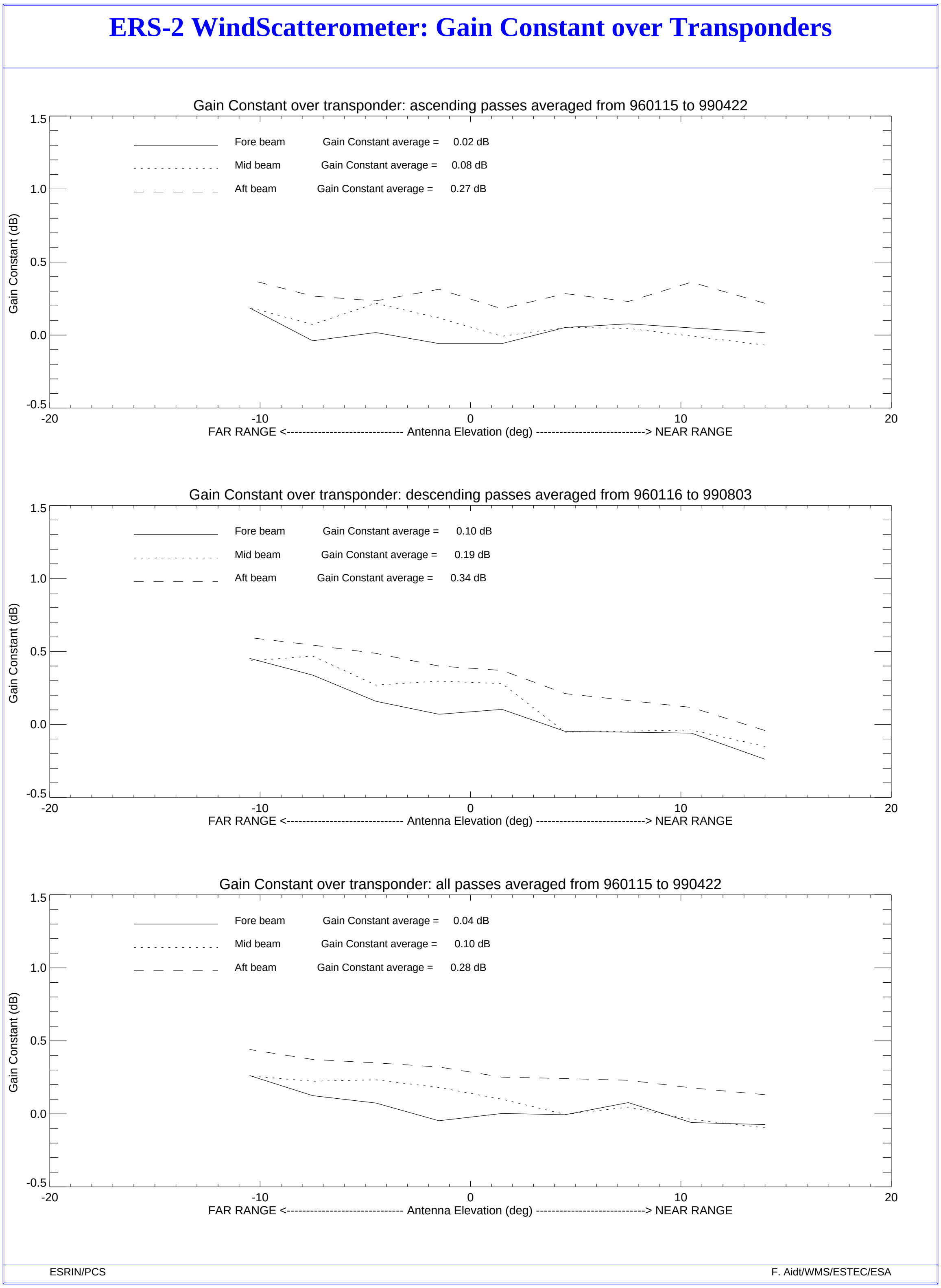

FIGURE 4. ERS-2 Scatterometer: gain constant over transponders plus a scaling factor. All data available since January 1996. Upper plot: ascending passes. Middle plot: descending passes. Lower plot: all passes.

2.2 Ocean Calibration

ECMWF performs the monitoring of ERS-2 sigma noughts over ocean (see the report in Annex).

The sigma nought bias is defined as the difference between the ERS-2 sigma-nought and the sigma nought retrieved using the CMOD-4 model with the First Guess at Appropriate Time (FGAT) background winds.

The sigma nought biases with respect to the ECMWF model first guess winds are similar to the results from the previous cycle. The antenna patterns show a flat profiles in particular for the near mid range. The biases are slight larger for incident angle above 45 degrees (fore and aft antennae).

2.3 Gamma-nought over Brazilian rain forest

Although the transponders give accurate measurements of the antenna attenuation at particular points of the antenna pattern, they are not adequate for fine tuning across all incidence angles, as there are simply not enough samples. The tropical rain forest in South America has been used as a reference distributed target. The target at the working frequency (C-band) of ERS-2 Scatterometer acts as a very rough surface, and the transmitted signal is equally scattered in all directions (the target is assumed to follow the isotropic approximation). Consequently, for the angle of incidence used by ERS-2 Scatterometer, the normalised backscattering coefficient (sigma-nought) will depend solely on the surface effectively seen by the instrument:

$$S^0 = S \bullet \cos\theta$$

With this hypothesis it is possible to define the following formula:

$$\gamma^0 = \frac{\sigma^0}{\cos\theta}$$

Using this relation, the gamma-nought backscattering coefficient over the rain forest is independent of the incident angle, allowing the measurements from each of the three beams to be compared.

The test area used by the PCS is located between 2.5 degrees North and 5.0 degrees South in latitude and 60.5 degrees West and 70.0 degrees West in longitude.

The following paragraphs give a description of the activities carried out with this natural target.

2.3.1 Antenna pattern: Gamma-nought as a function of elevation angle

This analysis is carried out by ESTEC that has selected a larger region than the one used as test area within PCS. In this case the selected rain forest extends from 2.0 degrees South to 11.0 degrees South in latitude and 56.0 degrees West to 80 degrees West in longitude. A large area is selected in order to have a larger amount of measurements.

For cycle 48 the antenna patterns as function of the elevation angle have not been computed by ESTEC.

2.3.2 Antenna pattern: Gamma-nought as a function of incident angle

Figure 5 shows the antenna patterns as a function of the incident angle for cycle 48.

The antenna patterns for the cycle 48 are very close to the ones obtained in the previous cycle. The small change in the average value is within the seasonal variation of the Amazon rain forest. The antenna patterns show a flat profile, within 0.3 dB for the descending passes and within 0.4dB for the ascending ones.

The monitoring of the antenna patterns shows a small slope at the near-mid range of the fore and aft antenna profile at ascending passes.

The mid antenna profile (at far range) is roughly 0.1 dB less than the fore and aft ones.

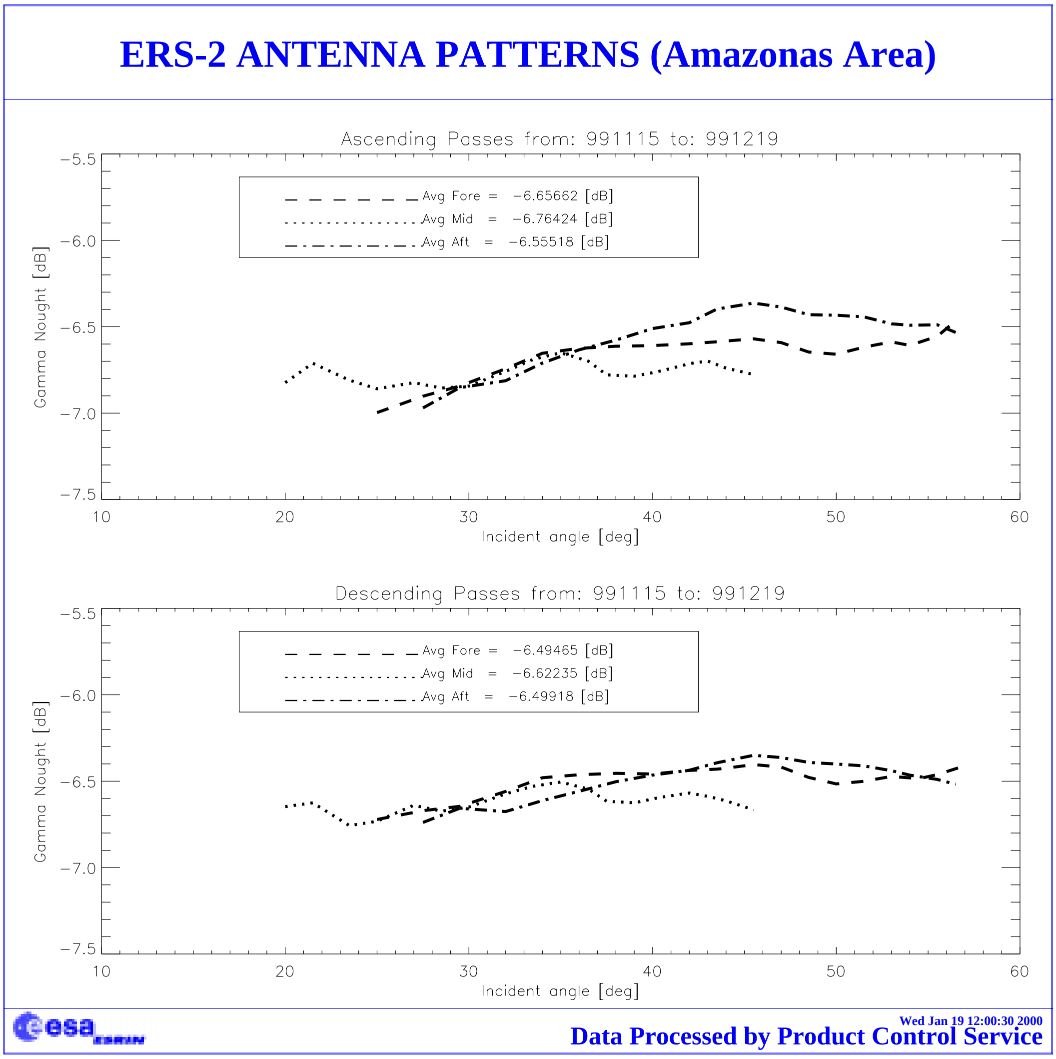

FIGURE 5. ERS-2 Scatterometer antenna patterns as function of the incident angle: cycle 48.

2.3.3 Gamma-nought histograms and peak position evolution

As the gamma-nought is independent from the incidence angle, the histogram of gamma-noughts over the rain forest is characterised by a sharp peak. The time-series of the peak position gives some information on the stability of the calibration. This parameter is computed by fitting the histogram with a normal distribution added to a second order polynomial:

$$F\langle x\rangle = A_0 \cdot \exp\left(-\frac{z^2}{2}\right) + A_3 + A_4 \cdot x + A_5 \cdot x^2$$

where: $z = \frac{x - A_1}{A_2}$

The parameters are computed using a non linear least square method called “gradient expansion”. The position of the peak is given by the maximum of the function F(x). The histograms are computed weekly (from Monday to Sunday) for each antenna individually (“Fore”, “Mid”, and “Aft”) and for ascending and descending passage with a bin size of 0.02 dB.

Figure 6 shows the evolution of the histograms peak position since January 1996. The step shown in March 1996 is due to the end of commissioning phase when a new Look Up Table was used in the ground stations for WSCATT FD-products generation. It is interesting to note the decrease of roughly 0.2 dB from August 1996 to June 1997. This is linked to the switch of the Scatterometer calibration subsystem from side A to side B on 6th of August. The redundancy of side A device caused a little change in the calibration that was corrected on 19^{th} June 1997 with a new calibration LUT used in the ground processing.

Figure 7 shows the evolution of the peak position corrected with the new calibration set also for the period from August 1996 to June 1997. From the plots in figure 7 it is clear that the calibration stability achieved over the rain forest is within 0.5 dB. A seasonal effect is also present in the peak position evolution for the three antennae.

For the interbeam calibration the results are shown in Figure 8. On average the peak values for the aft and fore antenna are very close together. The difference between the fore antenna signal and the mid antenna signal is roughly 0.1 dB (both ascending and descending passes) while the difference between the aft antenna signal and the mid antenna signal seems to have a seasonal behaviour. This differences is close to 0.1 dB during the summer and it is close to 0.2 dB during the winter for the ascending passes. For the descending passes the differences between the winter and the summer is less clear and the aft-mid interbeam calibration is around 0.15 dB.

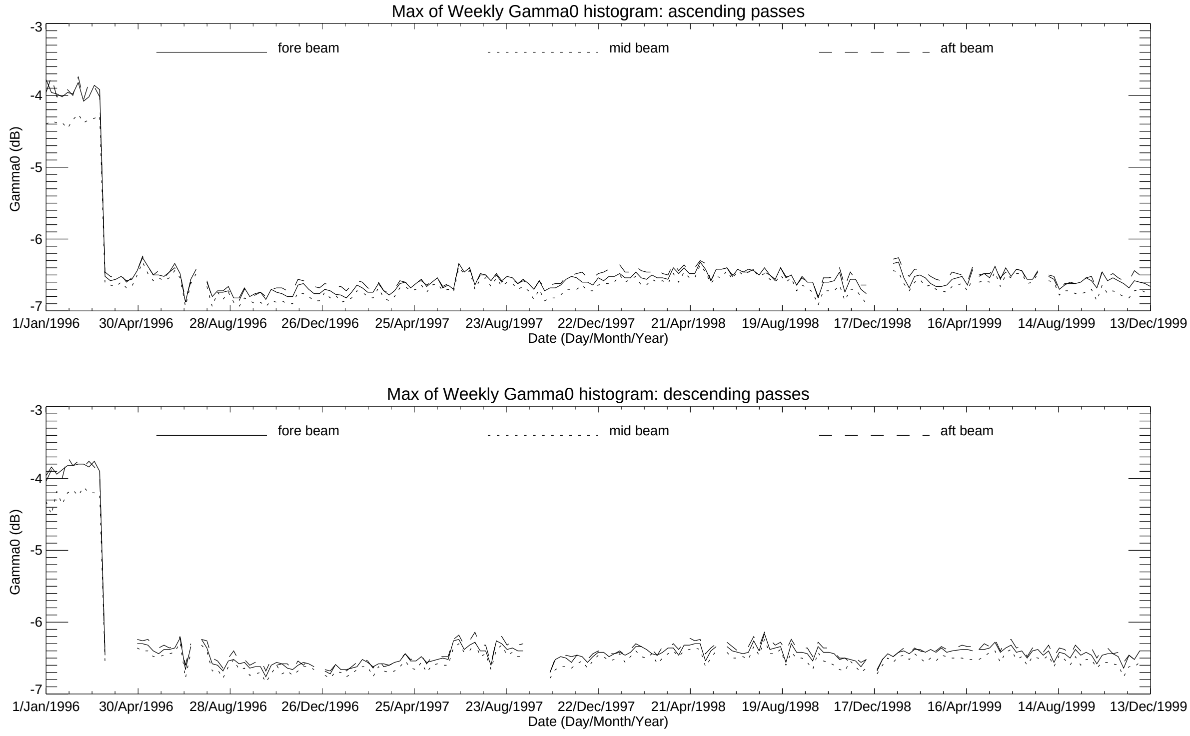

FIGURE 6. ERS-2 Scatterometer, gamma-nought histogram: weekly evolution of maximum position. From up to down: ascending passes, descending passes.

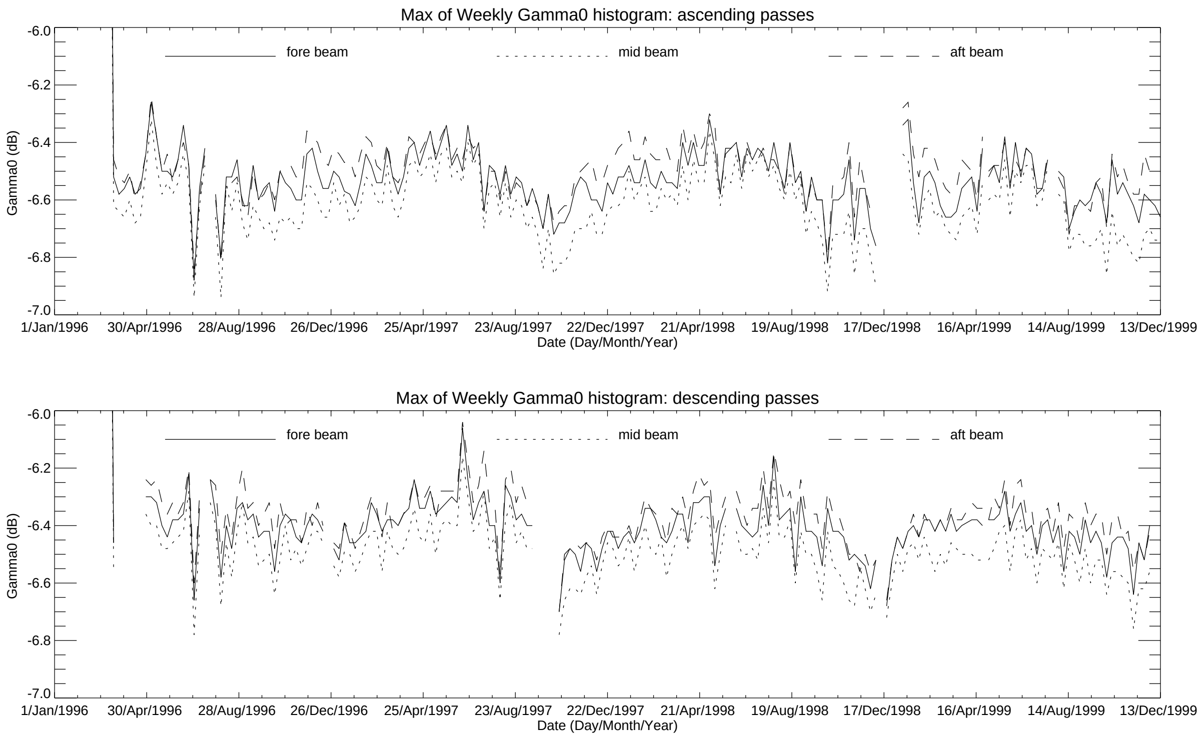

FIGURE 7. Gamma-nought histogram: weekly evolution of maximum position. Data from 6th of August 1996 to 19th June 1997 are corrected with the new calibration constant (+0.2dB). Upper plot: ascending passes. Lower plot: descending passes.

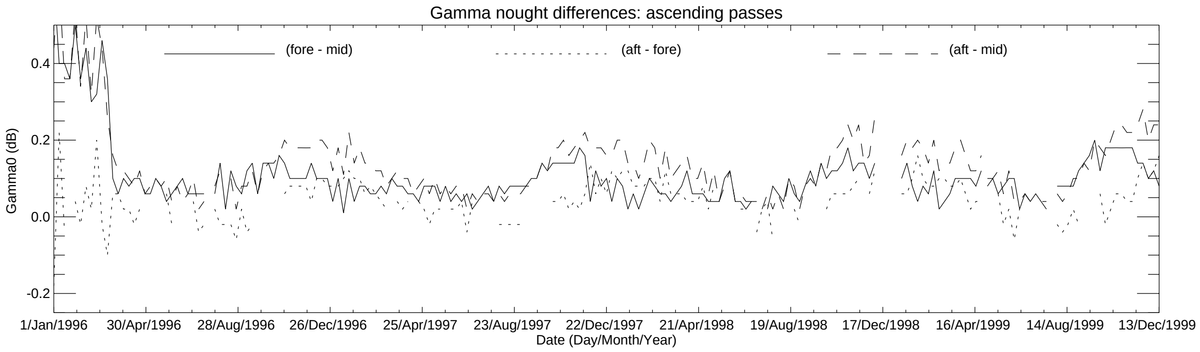

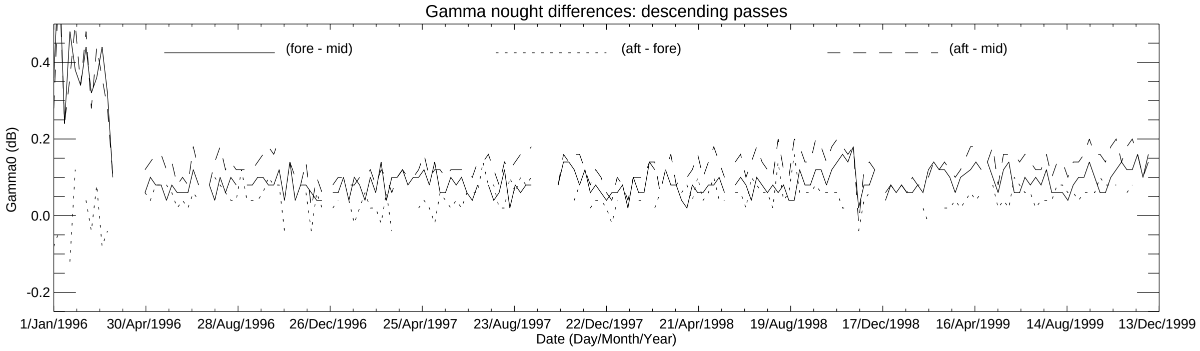

FIGURE 8. Interbeam calibration, weekly differences of the maximum position. From up to down: ascending passes, descending passes.

The mean and the standard deviation of gamma-nought are weekly computed directly using the Fast Delivery data. Figure 9 shows the evolution of the standard deviation since September 1996. The ascending passes show a gamma nought standard deviation more higher than the descending ones. This can be explained because at ascending passes the test site appears less homogeneous in particular for some areas near the rivers (see Figure 15). The last plot in Figure 9 shows the number of valid measurements used to compute the statistics. It is clear the reduction of the number of valid observation since the beginning of 1999. This is due to an increase of SAR images acquired over the Amazon rain forest.

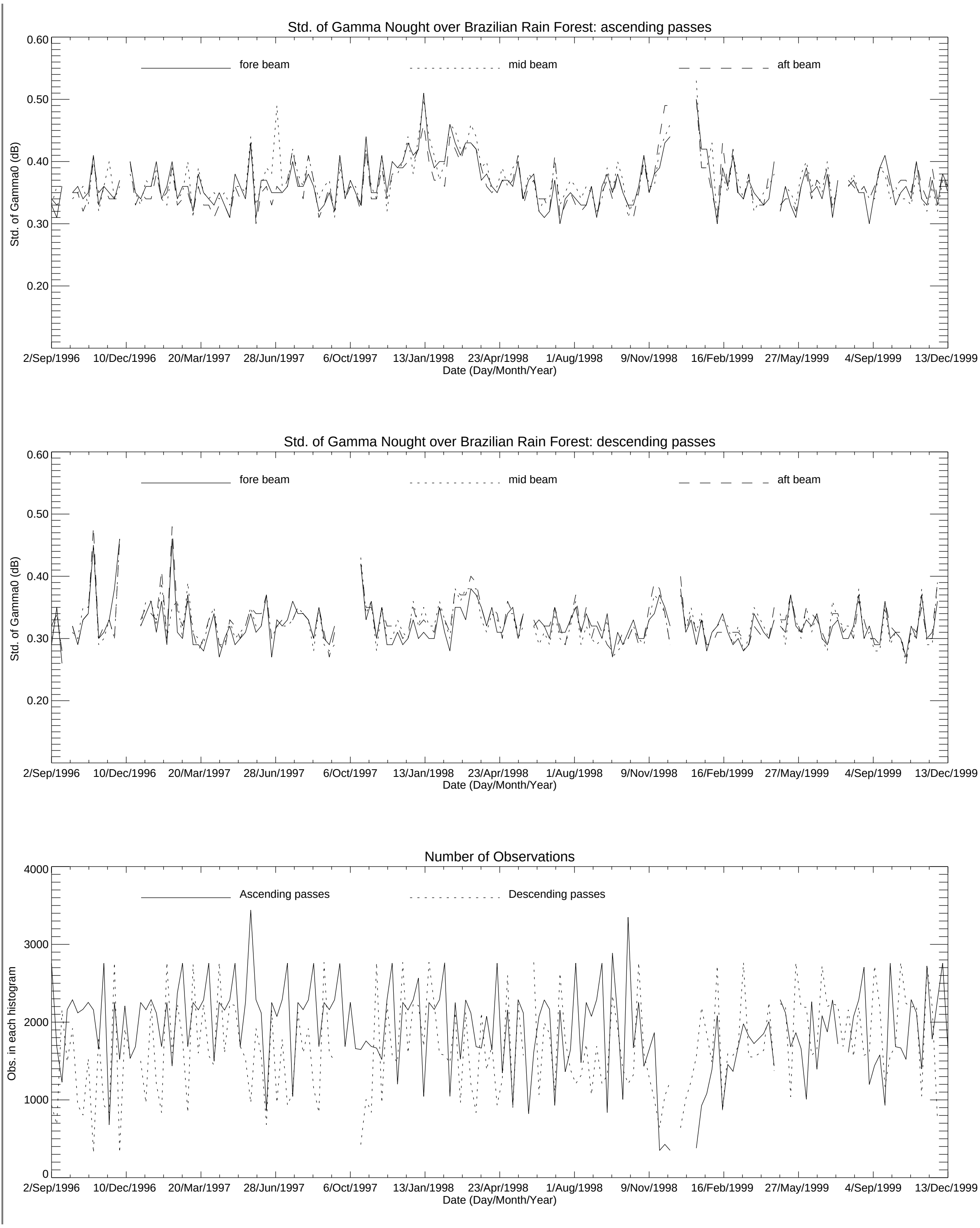

FIGURE 9. Gamma-nought histograms: weekly evolution of standard deviation. From up to down: ascending passes standard deviation, descending passes standard deviation, number of valid observations.

The Figures from 10 to 14 show the gamma-nought histogram over the Brazilian rain forest throughout cycle 48.

The shape of the histograms has a good quality. The histogram for descending passes are available only for the first two week. For the other weeks only a small number of data are available and therefore the histograms are not computed or they are not valid. The missing of the data during the descending passes is due to SAR acquisitions over the test area.

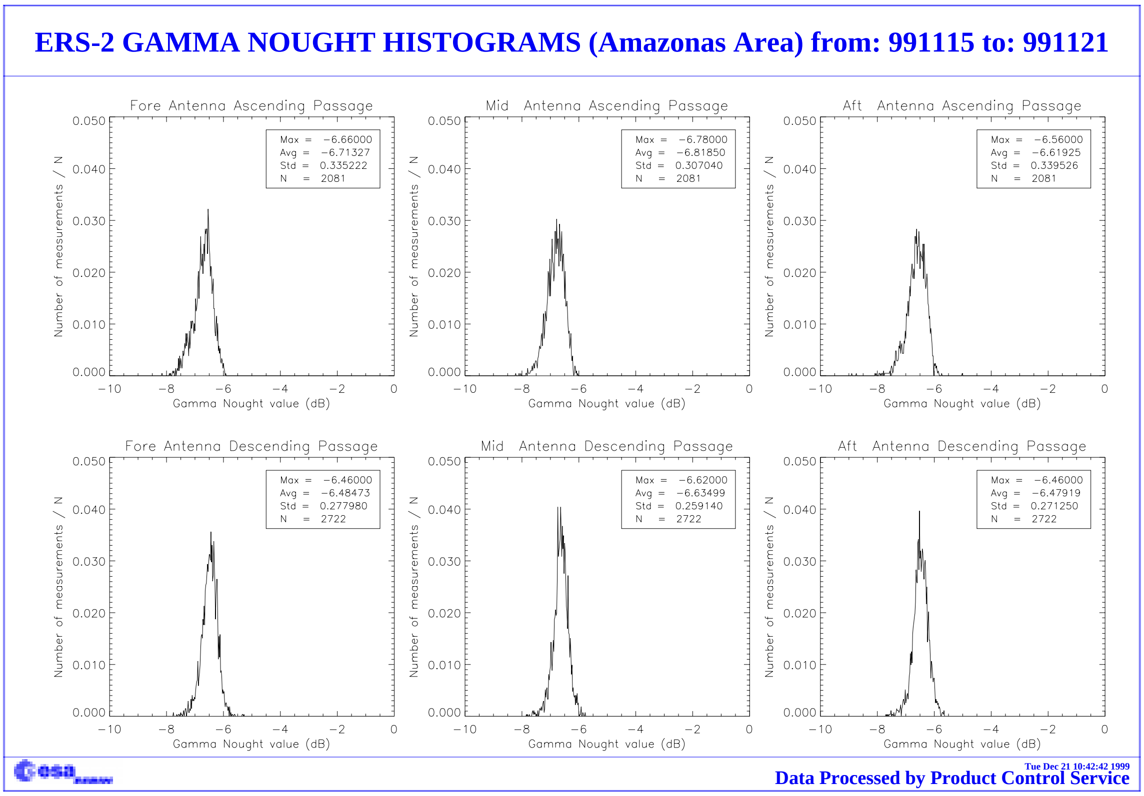

FIGURE 10. Gamma-nought histograms over Brazilian Rain forest: first week of the cycle 48

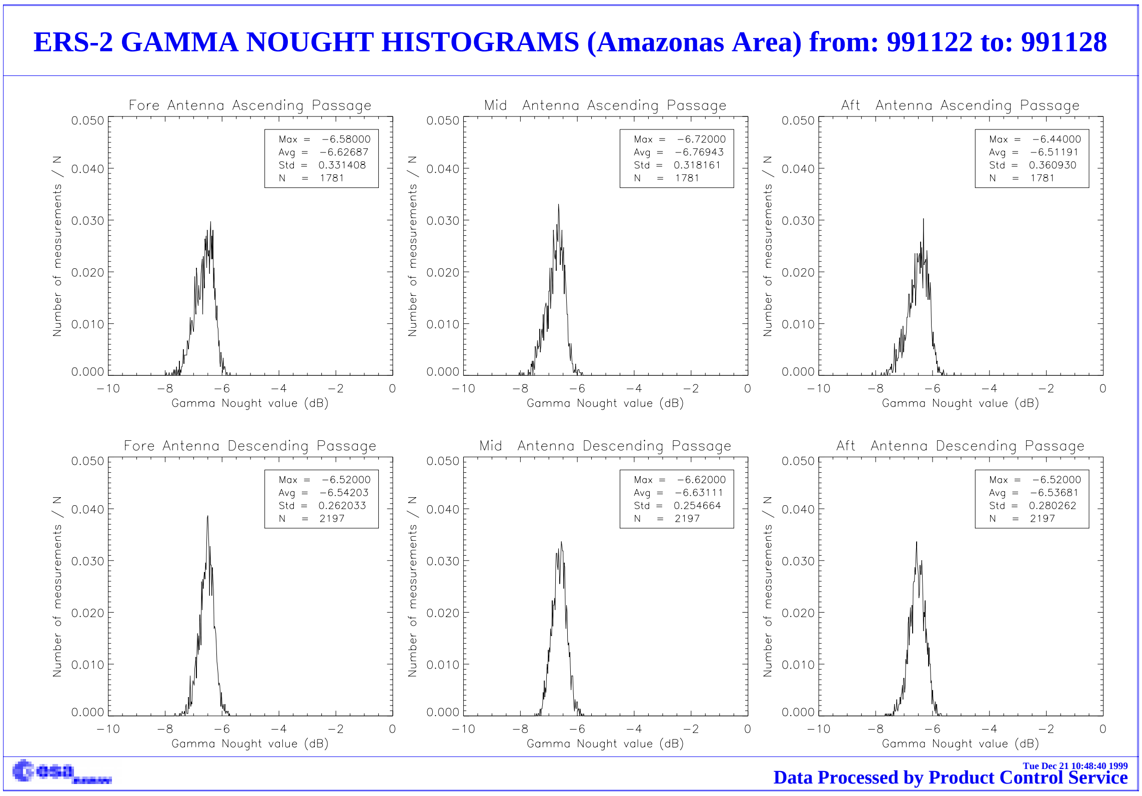

FIGURE 11. Gamma-nought histograms over Brazilian Rain forest: second week of the cycle 48

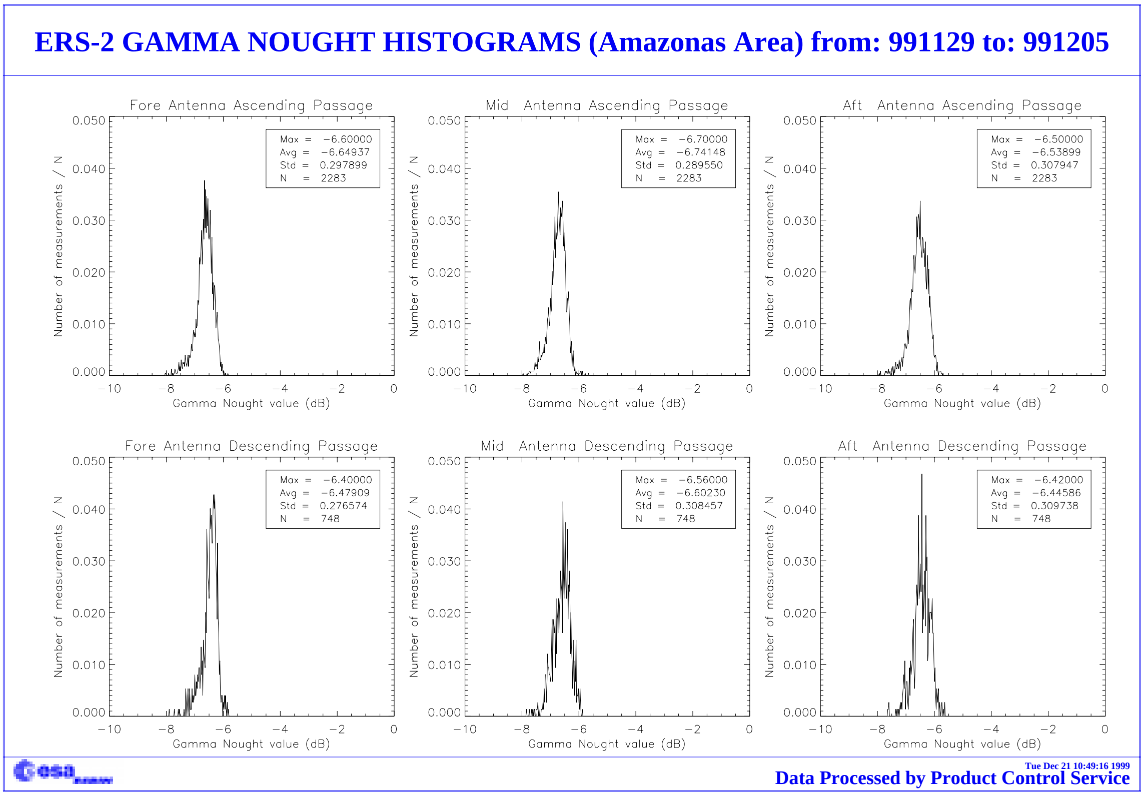

FIGURE 12. Gamma-nought histograms over Brazilian rain forest: third week of the cycle 48

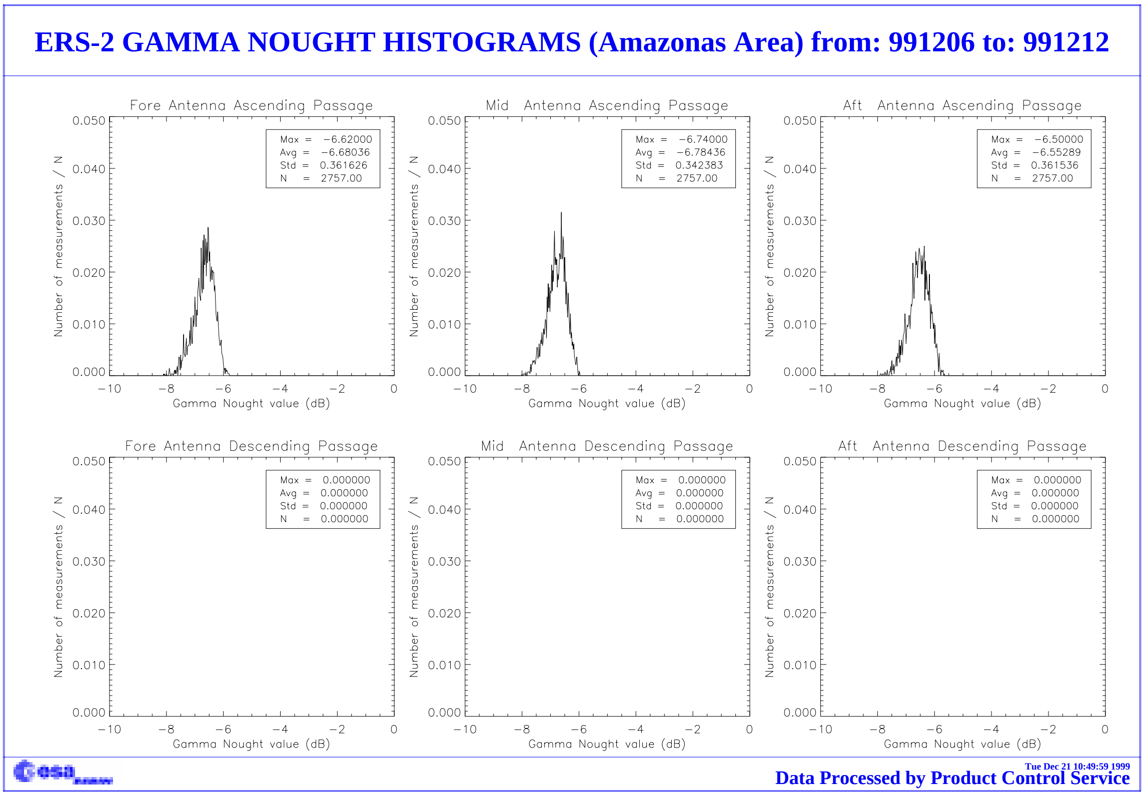

FIGURE 13. Gamma-nought histograms over Brazilian rain forest: fourth week of the cycle 48.

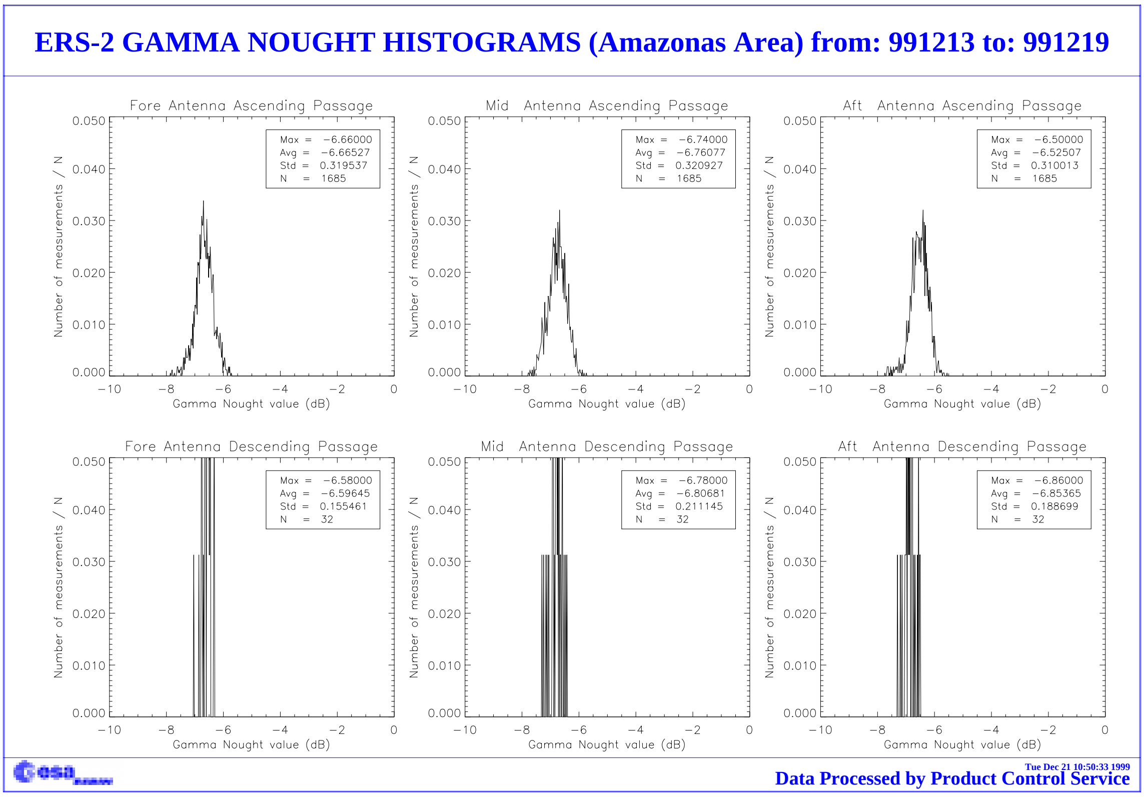

FIGURE 14. Gamma-nought histograms over Brazilian rain forest: fifth week of the cycle 48.

2.3.4 Gamma nought image of the reference area

The Figure 15 shows maps of the gamma nought over the Brazilian rain forest. This is the area where statistics are computed.

Each map has a resolution of 0.5 degrees in latitude and 0.5 degrees in longitude, roughly this is the instrument resolution at the latitude of the test site. In each resolution cell falls the average of all the valid observations available during one cycle (35 days).

From the figures no important changes happened in the test area during the cycle 48. As outlined in the previous reports the test area appears less homogenous at the ascending passes than in the descending ones. This seems due to the signal that comes from some areas near the rivers.

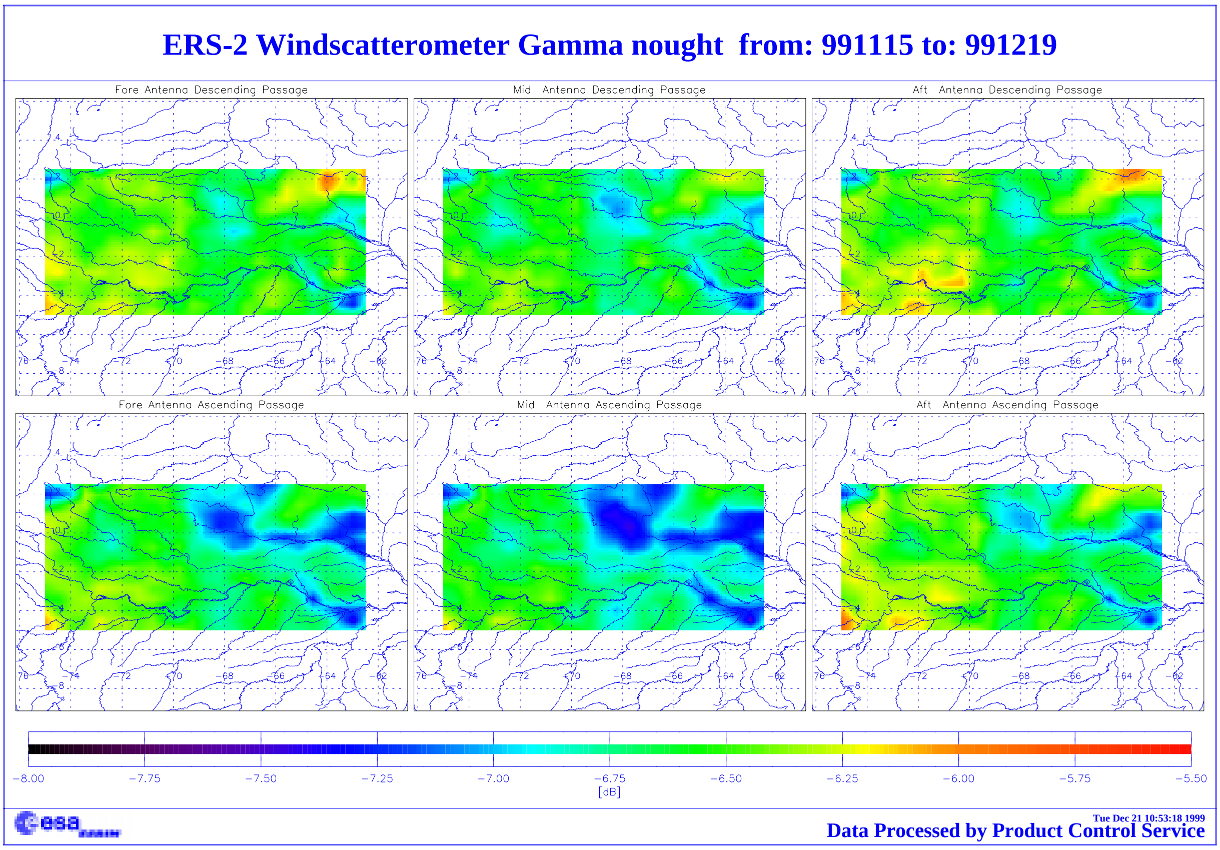

FIGURE 15. ERS-2 Scatterometer: gamma nought over the Brazilian rain forest cycle 48.

2.3.5 Antenna temperature evolution over the Rain Forest

The monitoring of the antenna temperature over the Brazilian rain forest is performed by PCS. The antenna temperatures are retrieved from the satellite telemetry when the Scatterometer swath is over the test site and the instrument is active (AMI in wind only or wind/wave mode). The scope of this monitoring is to investigate a possible correlation between the antenna temperatures and the gamma-nought level. This correlation is not clear in the actual data because of the gamma nought variability of the selected area. A deep analysis is to be performed to better understand the facts.

The plots for the three beams and for the ascending, descending and all passes are in Figure 16. It is interesting to note that the annual variation is due to the earth inclination and that the antenna temperatures have an increase of roughly 1.0 degree per year in the case of the mid and fore antenna; 2 degrees per year for the aft antenna.

This temperature increase could be related to the degradation of the antennae protection film.

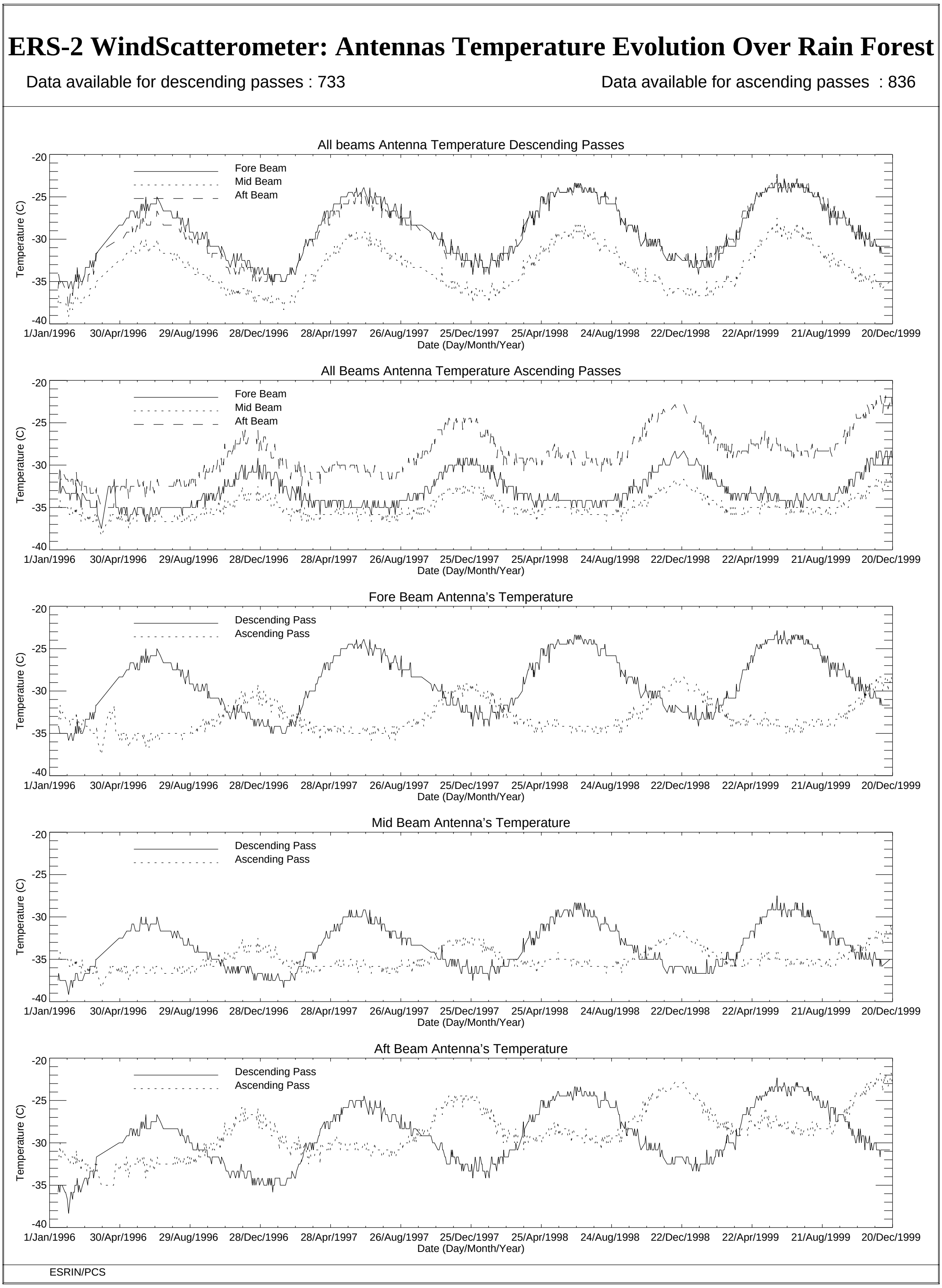

FIGURE 16. ERS-2 Scatterometer: evolution of the antenna temperatures over the Brazilian rain forest.

3.0 Instrument performance

The instrument status is checked by monitoring the following parameters:

- Centre of Gravity and standard deviation of the received signal spectrum. This parameter is useful for the monitoring of the orbit stability, the performances of the doppler compensation filter, the behaviour of the yaw steering mode and the performances of the devices in charge for the satellite attitude (e.g. gyroscopes, earth sensor).
- Noise power I and Q channel.
- Internal calibration pulse power.

the latter is an important parameter to monitor the transmitter and receiver chain, the evolution of pulse generator, the High Power Amplifier (HPA), the Travelling Wave Tube (TWT) and the receiver.

These parameters are extracted daily from the UWI products and averaged. The evolution of each parameter is characterised by a least square line fit. The coefficients of the line fit are printed in each plot.

3.1 Centre of gravity and standard deviation of received power spectrum

The Figure 17 shows the evolution of the two parameters for each beam. The tendency since the beginning of the mission is a clear increase of the Centre of gravity (CoG) of the signal spectrum for the three antennae while the result for the standard deviation is more stable apart from the change occurred on 26th, October 1998. On October 26th, 1998 the standard deviation of the CoG had, on average, a decrease of roughly 100 Hz for the fore and aft antenna and of roughly 30Hz for the mid antenna. This change is linked with the increase of the transmitted power (see 3.3).

The two steps observed on the plots of the CoG (see Figure 17) are due to a change in the pointing subsystem (DES reconfiguration) side B instead of side A after a depointing anomaly (see table 2 for the list of the AOCS depointing anomaly occurred during the ERS-2 mission). The first change is from 24th, January 1996 to 14th, March 1996, the second one is from 14th February 1997 to 22nd April 1997. During these periods side B was switched on. It is important to note that during the first time a clear difference in the CoG is present only for the Fore antenna (an increase of roughly 100 Hz) while during the second time the change has affected all the three antennae (roughly an increase of 200 Hz, 50 Hz and 50 Hz for the fore, mid and aft antenna respectively).

Table 2: ERS-2 Scatterometer AOCS depointing anomaly

From	To
24th January 1996 9:10 a.m.	26th January 1996 6:53 p.m
14th February 1996 1:25 a.m.	15th February 1996 3:44 p.m
3rd June 1998 2:43 p.m.	6th June 1998 12:47 a.m.
1st September 1999 8:50 a.m.	2nd September 1999 1:28 a.m.

The large deviations from the nominal values in the plots of the CoG of the fore and aft antenna are due to the missing of the Yaw Steering Mode or are due to the missing of the on board doppler coefficients as reported in Table 3.

Table 3: ERS-2 Scatterometer anomalies in the CoG fore and aft antenna

Date	Reason
26th and 27th September 1996	missing on-board doppler coefficient (after cal. DC converter test period)
6th and 7th June 1998	no Yaw Steering Mode (after depointing anomaly)
2nd and 3rd December 1998	missing on-board doppler coefficients (after AMI anomaly 228)

The peaks shown in the plot of mid beam CoG standard deviation are linked to the satellite manoeuvres and the DES reconfiguration.

For the cycle 48 the evolution of the doppler compensation has been within the nominal range as shown in Figure 18. The large peak on 8th December 1999 is due to an orbit manoeuvre.

ERS-2 WindScatterometer: DOPPLER COMPENSATION Evolution (UWI)

Least-square poly. fit fore beam Center of gravity = -301.2 +(0.0938)*day Standard Deviation = 4242.1 +(0.0560)*day
Least-square poly. fit mid beam Center of gravity = -645.8 +(0.1050)*day Standard Deviation = 5129.4 +(0.0069)*day
Least-square poly. fit aft beam Center of gravity = -362.3 +(0.0910)*day Standard Deviation = 4368.1 +(0.0401)*day

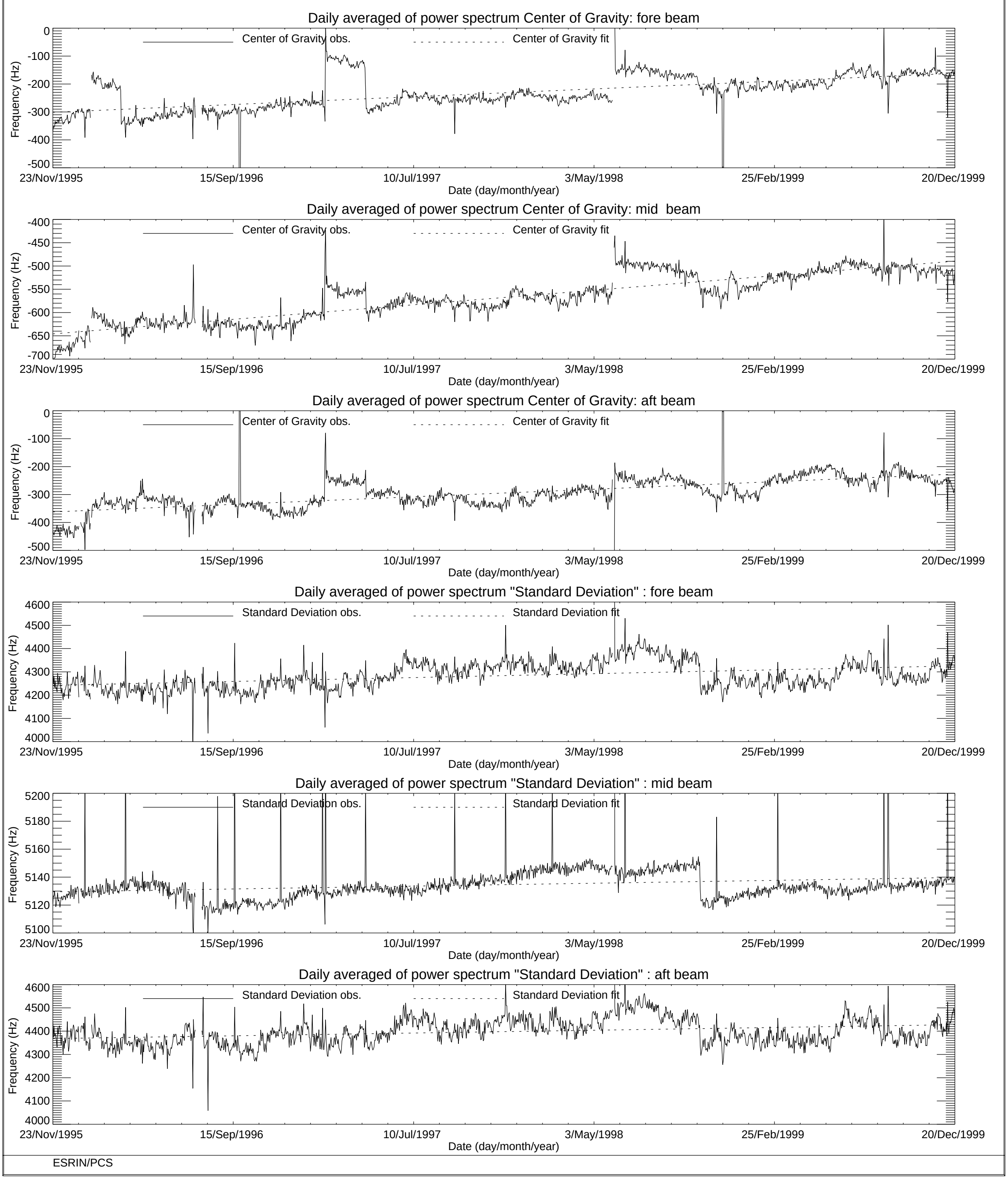

FIGURE 17. ERS-2 Scatterometer: Centre of Gravity and standard deviation of received power spectrum since the beginning of the mission.

ERS-2 WindScatterometer: DOPPLER COMPENSATION Evolution (UWI)

Least-square poly. fit fore beam	Center of gravity = -156.1 +(-0.156)*day	Standard Deviation = 4257.4 +(1.2902)*day
Least-square poly. fit mid beam	Center of gravity = -506.6 +(-0.175)*day	Standard Deviation = 5132.2 +(0.1442)*day
Least-square poly. fit aft beam	Center of gravity = -231.1 +(-0.598)*day	Standard Deviation = 4351.8 +(1.5933)*day

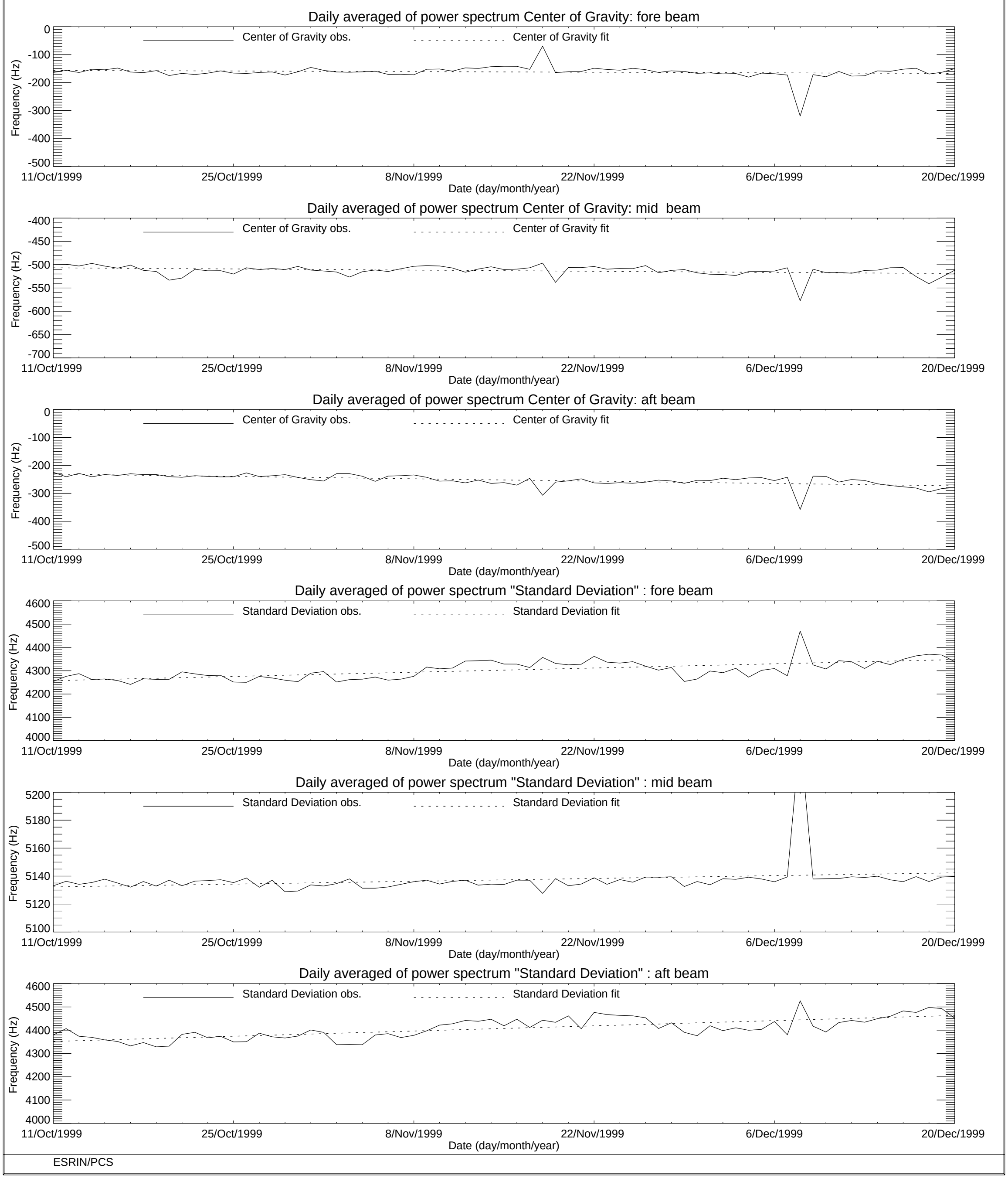

FIGURE 18. ERS-2 Scatterometer: Centre of Gravity and standard deviation of received power spectrum cycle 47 and cycle 48.

3.2 Noise power level I and Q channel

The results of the monitoring are shown in Figure 19. The first set of three plots presents the noise power evolution for the I channel while the second set shows the Q channel. The noise level is less than 1 ADC Unit for the fore and aft signals and is negligible for the mid one. From the plots one can see that the noise level is more stable in the I channel than in the Q one. The PCS suspects that an explanation should be found in the different position of the receivers, in particular it seems that the Q one is closer to the ATSR-GOME electronics. A confirmation of this hypothesis has been asked to ESTEC.

Since 5th December 1997 some high peaks appear in the plots. These high values for the daily mean are due to the presence for these special days of a single UWI product with an unrealistic value in the noise power field of the Specific Product Header. The analysis of the raw data used to generate these products lead in all cases to the presence of one source packet with a corrupted value in the noise field stored into the source packet Secondary Header. Table 4 presents the list of the UWI products affected by a corrupted noise field and disseminated during cycle 48.

Table 4: UWI products with noise field corrupted (cycle 48)

Noise Field corrupted	Noise value (ADC Unit)	Acquisition Time
None	-	-

The reason why noise field corruption is beginning from 5th December 1997 is at present unknown. It is interesting to note that at the beginning of December 1997, we started to get as well the corruption of the Satellite Binary Times (SBTs) stored in the EWIC product. The impact in the fast delivery products was the production of blank products starting from the corrupted EWIC until the end of the scheduled stop time. A change in the ground station processing in March 1998 overcame this problem.

Since 9th August 1998 some periods with a clear instability in the noise power have been recognised. Table 5 gives the detailed list.

Table 5: ERS-2 Scatterometer instability in the noise power

From	To
9th August 1998	26th October 1998
29th November 1998	6th December 1998
23rd December 1998	24th December 1998
7th June 1999	10th June 1999
17th August 1999	22nd August 1999
8th September 1999	9th September 1999
3rd October 1999	8th October 1999
16th October 1999	18th October 1999
26th October 1999	28th October 1999

To better understand the instability of the noise power the PCS has carried out investigations in the scatterometer raw data (EWIC) to compute the noise power with more resolution. The result is that for the orbits affected by the instability the noise power had a decrease of roughly 0.7 dB for the fore and aft signals and a decrease of roughly 0.6 dB in the mid beam case (see report cycle 42). The decrease of the noise power during the orbits affected by the instability is comparable with the decrease of the internal calibration level that occurred during the same orbits. The reason of this instability (linked to the AMI anomalies) is still under investigation. A plot that shows the correlation among the noise power, the internal calibration level and the AMI anomaly is reported in section 3.3.

Figure 20 shows the evolution of the noise power since 26th October when 2 dB were added to the transmitted power. The periods with the instability in the noise are clear recognised.

During cycle 48 the evolution of the noise power was stable.

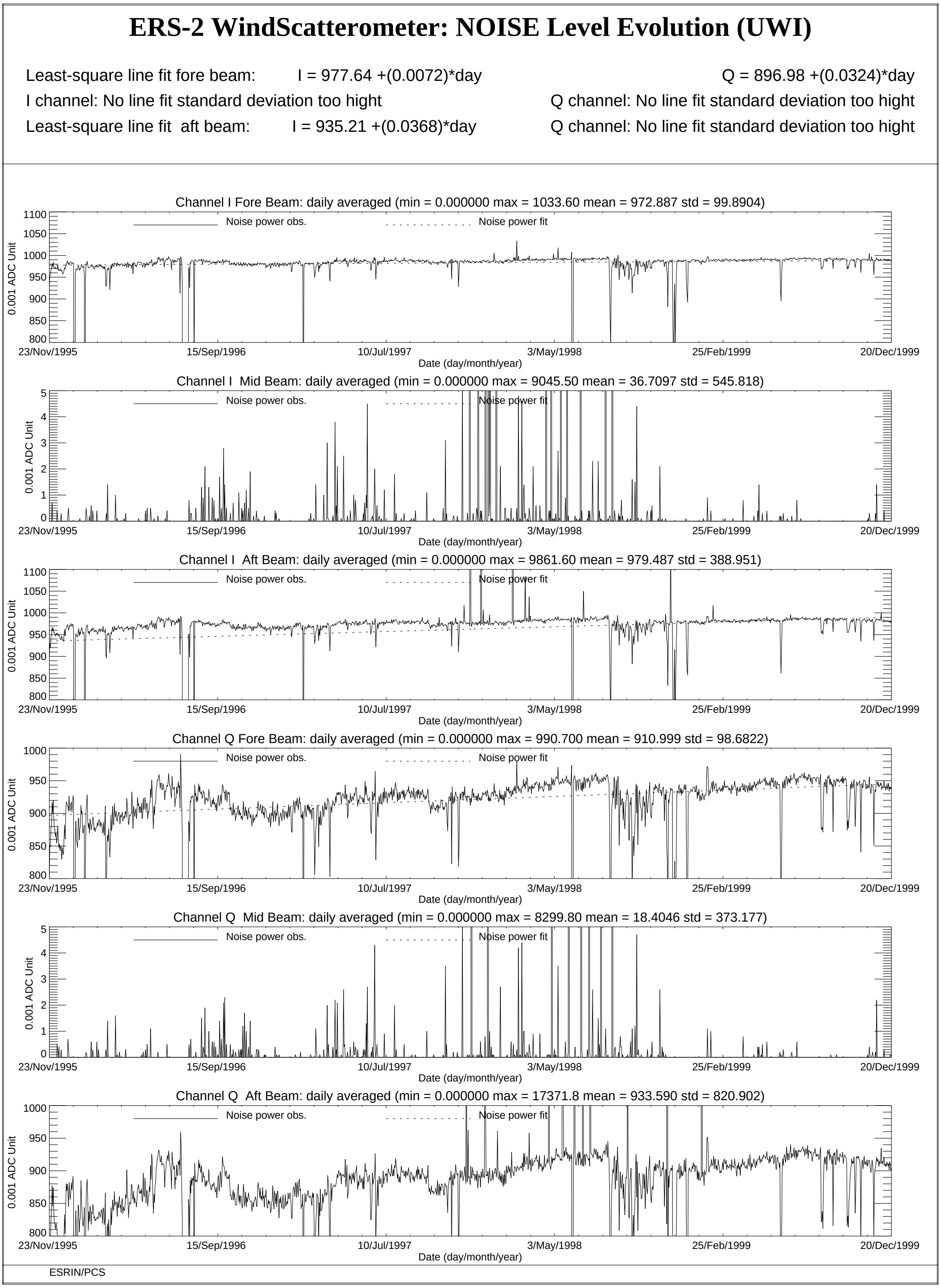

FIGURE 19. ERS-2 Scatterometer: noise power I and Q channel since the beginning of the mission.

ERS-2 WindScatterometer: NOISE Level Evolution (UWI)

Least-square line fit fore beam:	I = 986.46 +(0.0090)*day	Q = 932.90 +(0.0267)*day
Least-square line fit mid beam:	I = 0.0090 +(1.1804)*day	Q = 0.0096 +(2.6271)*day
Least-square line fit aft beam:	I = 978.00 +(0.0118)*day	Q channel: No line fit standard deviation too hight

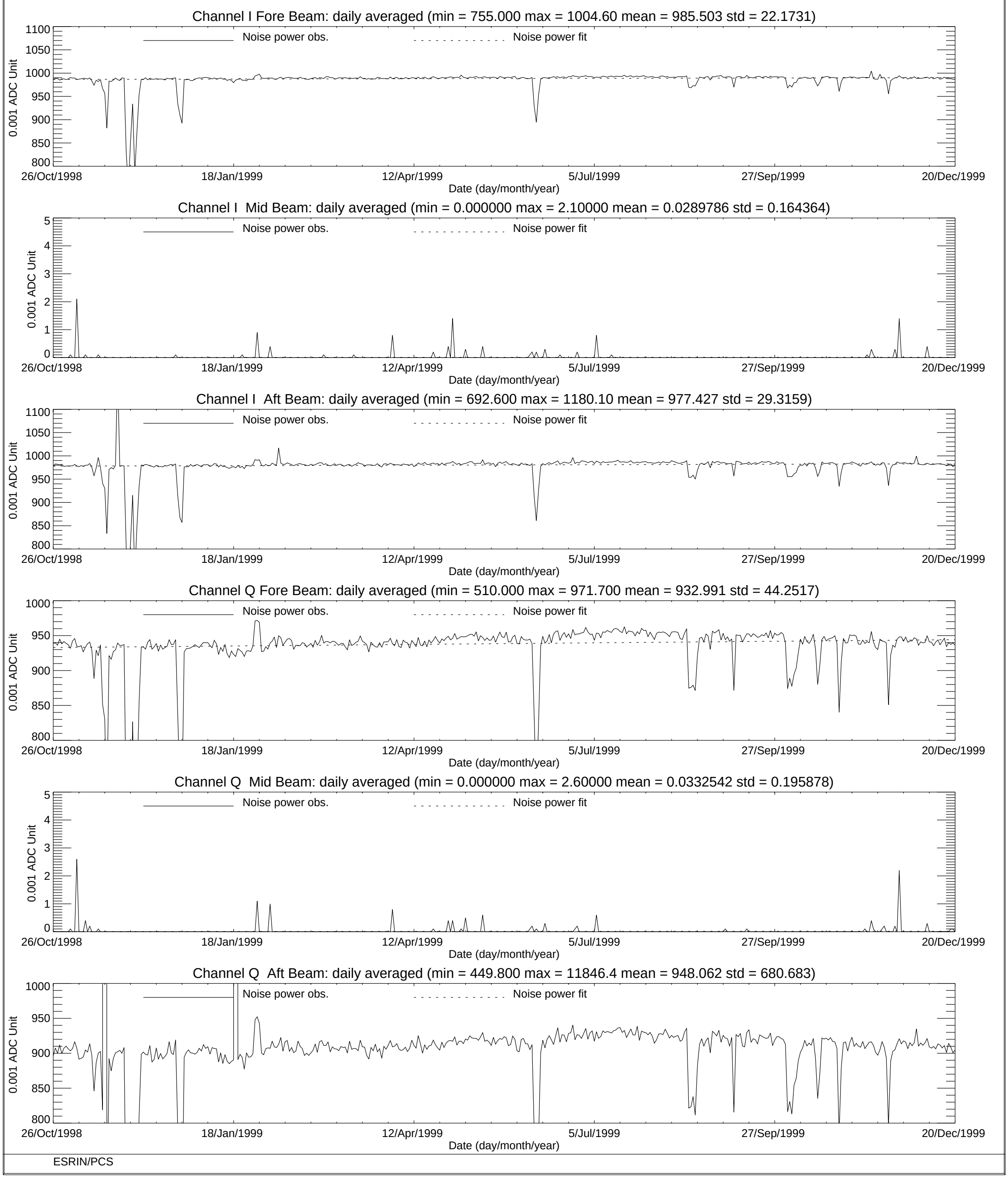

FIGURE 20. ERS-2 Scatterometer: noise power I and Q channel since 26th October 1998 when the transmitted power was increased by 2 dB.

3.3 Power level of internal calibration pulse

For the internal calibration level, the results, since the beginning of the mission, are shown in Figure 22.

The high value of the variance in the fore beam until August, 12th 1996 is due to the ground processing. In fact all the blank source packets ingested by the processor were recognized as fore beam source packets with a default value for the internal calibration level. The default value was applicable for ERS-1 and therefore was not appropriate for ERS-2 data processing. On August 12th, 1996 a change in the ground processing LUT overcame the problem.

Since the beginning of the mission a power decrease is detected. The reason is that the TWT is not working in saturation, so that a variation in input signal is visible in output. The variability of the input signal can be two-fold: the evolution of the pulse generator or the tendency of the switches between the pulse generator and the TWT to reset themselves into a nominal position. These switches were set into an intermediate position in order to put into operation the scatterometer instrument (on 16th November 1995). The decrease is estimated to be about 0.0025 dB per day. After the change of the calibration subsystem on August 6th, 1996 the decrease is more evident and it is estimated in 0.09 dB per cycle. The power decrease is regular and affects the AMI when it is working in wind-only mode, wind/wave mode and image mode indifferently.

On 26th October 1998 to compensate for this decrease, 2.0 dB were added to the Scatterometer transmitted power and this explains the large step shows in Figure 21 and Figure 22. After that day the power decrease is on average 0.07 dB per cycle.

It is important to point out the efficiency of the internal calibration for keeping the absolute calibration level stable. In fact, no important change is noted in the monitoring of the gamma-nought level over the Brazilian rain forest during the power decrease and after the increase of the transmitted power (see section 2.0).

The internal calibration level shows an instability since 9th August 1998 that is very well correlated with the instability in the noise power as outlined in section 3.2.

Figure 21 shows the daily average of the internal calibration and the noise power from 1st August 1998 to 20th December 1999. In the figure are also reported the anomalies that affected the AMI (the triangles in the plot) and the days when the instability was very strong (asterisks in the plot). From Figure 21 it seems that there is a clear correlation between the instability and the AMI anomalies.

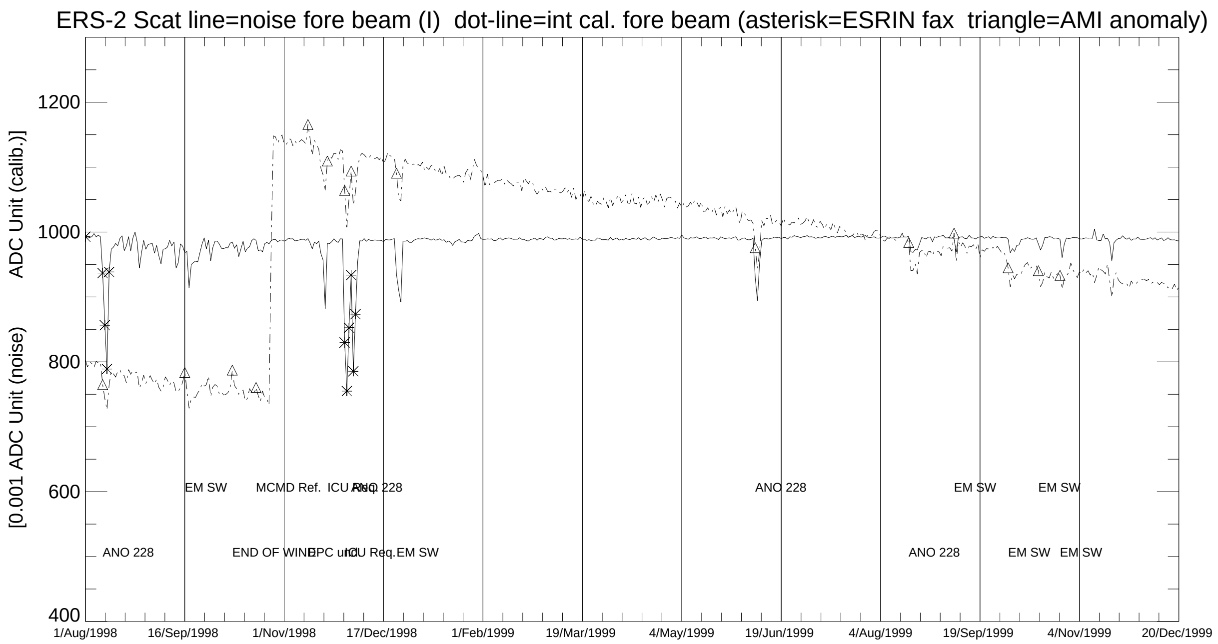

FIGURE 21. ERS-2 Scatterometer: noise power (I channel fore antenna) and internal calibration power (fore antenna) evolution from 1st August 1998 to 20th December1999.

During the cycle 48 the internal calibration level had, on average, a power decrease of 0.06 dB.

Apart from the AMI anomalies the power decrease since 26th October 1998 is regular and it is on average 0.07 dB per cycle as shown in Figure 23.

ERS-2 WindScatterometer: Internal CALIBRATION Level Evolution (UWI)

Least-square polynomial fit fore beam	gain (dB) per day -0.0001	1041.36 +(-0.0339394)*day
Least-square polynomial fit mid beam	gain (dB) per day -0.0001	305.190 +(-0.00795012)*day
Least-square polynomial fit aft beam	gain (dB) per day -0.0001	1021.79 +(-0.0290664)*day

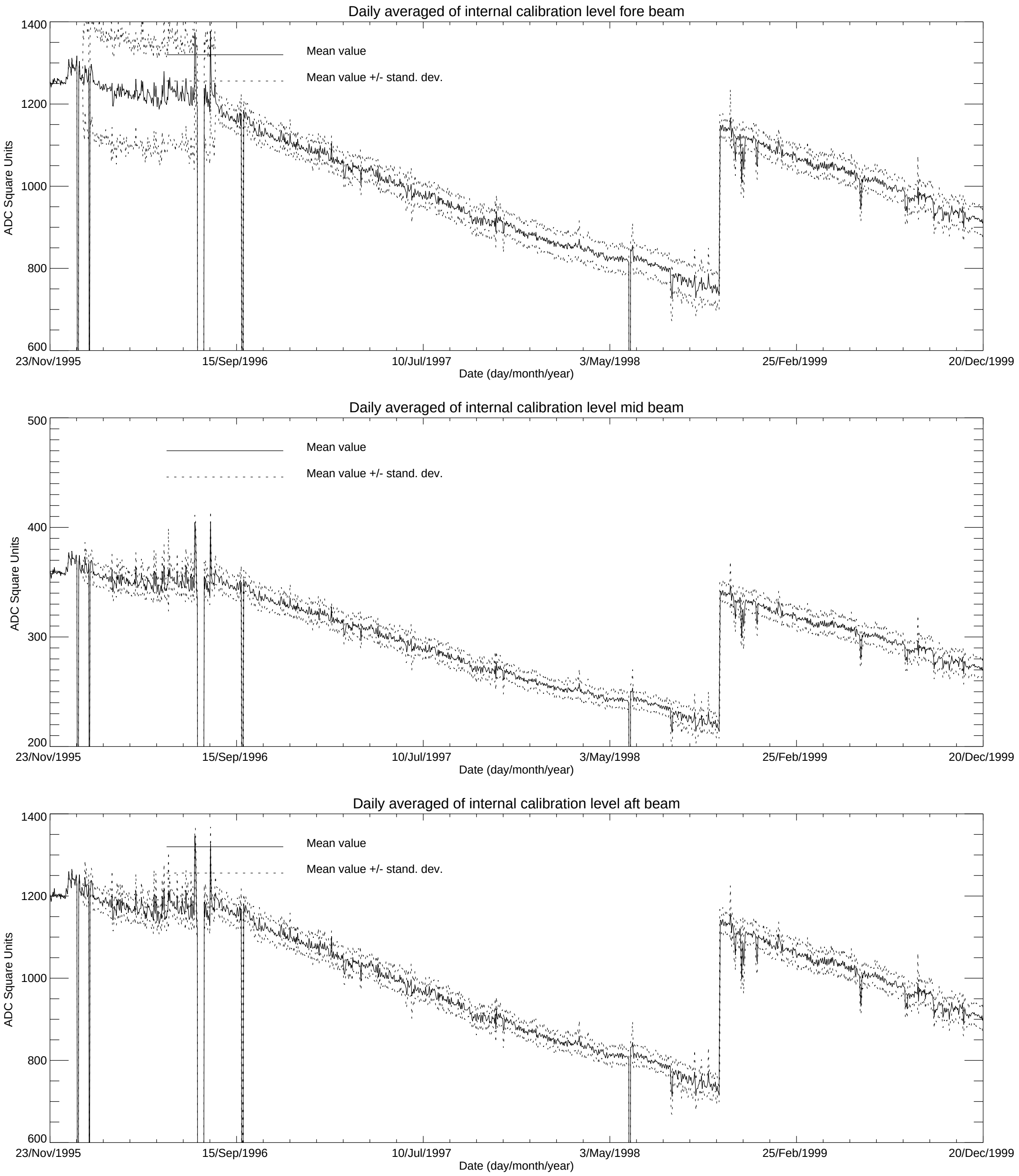

ESRIN/PCS

FIGURE 22. ERS-2 Scatterometer: power of internal calibration pulse since the beginning of the mission.

ERS-2 WindScatterometer: Internal CALIBRATION Level Evolution (UWI)

Least-square polynomial fit fore beam	gain (dB) per day -0.0021	1128.32 +(-0.496764)*day
Least-square polynomial fit mid beam	gain (dB) per day -0.0022	335.866 +(-0.150414)*day
Least-square polynomial fit aft beam	gain (dB) per day -0.0022	1120.85 +(-0.502773)*day

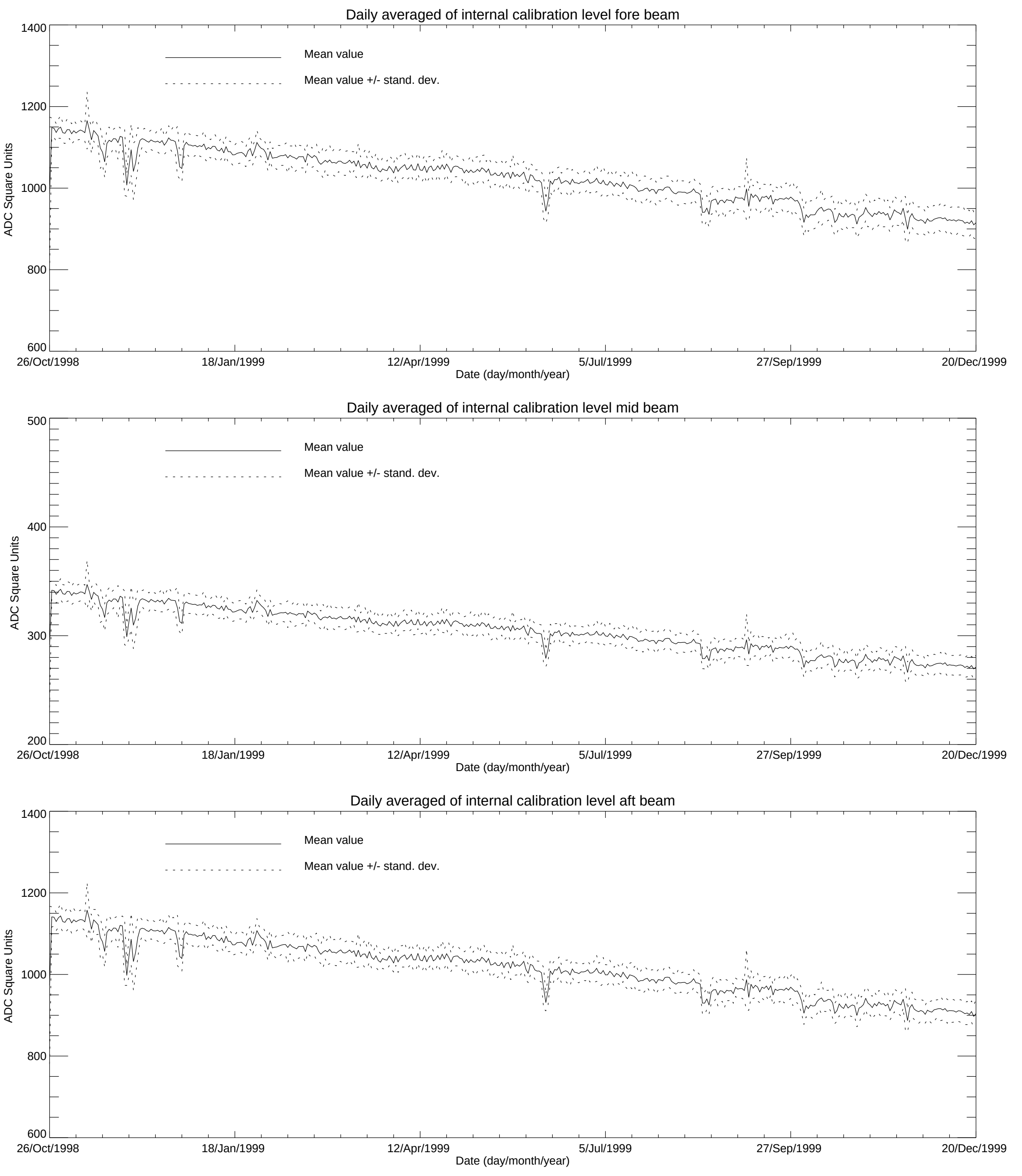

ESRIN/PCS

FIGURE 23. ERS-2 Scatterometer: power of internal calibration level since 26th October 1998 when the transmitted power was increased by 2.0 dB.

4.0 Products performance

One of the most important point in the monitoring of the products performance is their availability. The Scatterometer is a part of ERS payload and it is combined with a Synthetic Aperture Radar (SAR) into a single Active Microwave Instrument (AMI). The SAR users requirements and the constraints imposed by the on-board hardware (e.g. amount of data that can be recorded in the on-board tape) set rules in the mission operation plan.

The principal rules that affected the Scatterometer instruments are:

- over the Ocean the AMI is in wind/wave mode (scatterometer with small SAR imagettes acquired every 30 sec.) and the ATSR-2 is in low rate data mode.
- over the Land the AMI is in wind only mode (only scatterometer) and the ATSR-2 is in high rate mode. (Due to on board recorder capacity, ATSR-2 in high rate is not compatible with Sar wave imagette acquisitions.)

This strategy preserves the Ocean mission.

Moreover:

- the SAR images are planned as consequence of users' request.

These rules have an impact on the Scatterometer data availability as shown in Figure 24.

Each segment of the orbit has different colour depending on the instrument mode: brown for wind only mode, blue for wind-wave mode and green for image mode. The red and yellow colours correspond to gap modes (no data acquired). The major problems came from the orbit segments between Australia and Antarctic and between Africa and Antarctic where a lot of data are not acquired. This problem is under investigation by ESRIN and a new mission operation plan for the scatterometer shall be adopted.

For cycle 48 the percentage of the ERS-2 AMI activity is shown in table 6.

Table 6: ERS-2 AMI activity (cycle 48)

AMI modes	ascending passes	descending passes
Wind and Wind-Wave	**91.4%**	**82.7%**
Image	**1.3%**	**7.3%**
Gap and others	**7.3%**	**10.0%**

The percentage of scatterometer activity during the cycle 48 was within the nominal value. With reference to the cycle 47 there is a little increase of the percentage of wind operation during the ascending passes.

Table 7 reports the major data lost due to the test periods and AMI or satellite anomalies occurred after August 6th, 1996 (before of this day for many times data were not acquired due to the DC converter failure).

Table 7: ERS-2 Scatterometer mission major data lost after 6th, August 1996

From	To	Reason
September 23rd, 1996	September 26th, 1996	Test period
February 14th, 1997	February 15th, 1997	Depointing anomaly
June 3rd, 1998	June 6th, 1998	Depointing anomaly
November 17th, 1998	November 18th, 1998	ERS-2 switched off to face out Leonide meteo storm
September 22nd 1999	September 23rd 1999	Year 2000 certification test
November 17th, 1999	November 18th, 1999	ERS-2 switched off to face out Leonide meteo storm

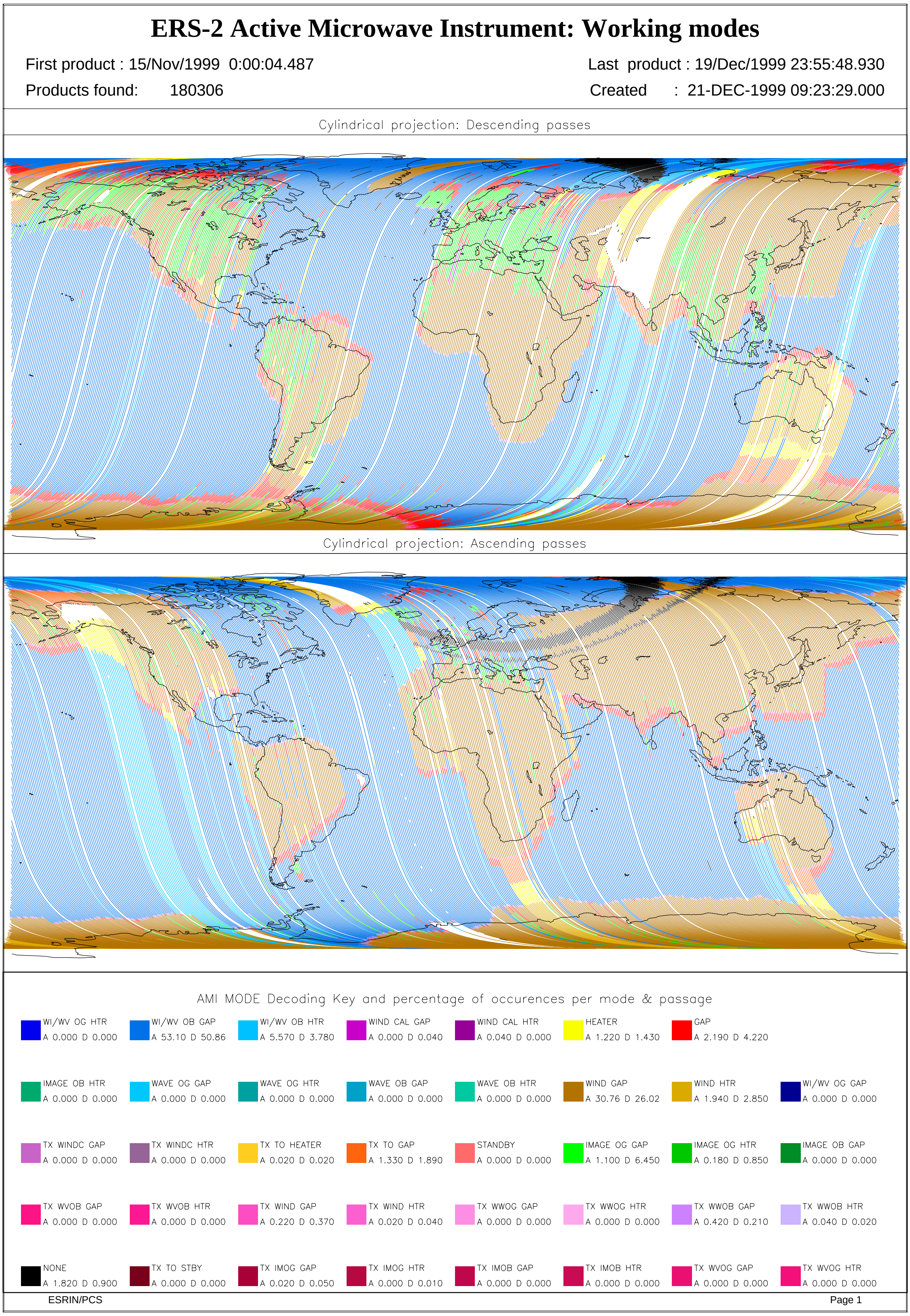

FIGURE 24. ERS-2 AMI activity during cycle 48.

The PCS carries out a quality control of the winds generated from the WSCATT data. The activity is split in two main areas: the first one includes a routine analysis of the fast Delivery Products disseminated to the users, the second one is focused on the improvement of the CMOD-4 (the operative ESA wind retrieval algorithm) for high wind speed (for more information see on theWeb site http//pcswww.esrin.esa.it the Cyclone Tracking home page). External contributions to this quality control come also from ECMWF and UK-Met Office.

The routine analysis is summarized in the plots of figure 25; from top to bottom:

- the monitoring of the valid sigma-nought triplets per day.
- the evolution of the wind direction quality. The ERS wind direction (for all nodes and only for those nodes where the ambiguity removal has worked properly) is compared with the ECMWF forecast. The plot shows the percentage of nodes for which the difference falls in the range -90.0, +90.0 degrees.
- the monitoring of the percentage of nodes whose ambiguity removal works successfully.
- the comparison of the wind speed deviation: (bias and standard deviation) with the ECMWF forecast.

The results since the beginning of the mission can be summarized (after August 6th, 1996 and apart from the events given in Table 7) as:

- a stable number of valid sigma-nought with a small increase after June 29th, 1999 due to the dissemination in fast delivery of the data acquired in the Prince Albert station.
- an accurate wind direction for roughly 93% of the nodes, a success in the ambiguity removal for more than 90.0% of the nodes.

The ERS-2 wind speed shows an absolute bias of roughly 0.5 m/s and a standard deviation that ranges from 2.5 m/s to 3.5 m/s with respect to the ECMWF forecast. The wind speed bias and its standard deviation have a seasonal pattern due to the different winds distribution between the winter and summer season.

It is important to note that only after the end of calibration phase (mid March 1996) the wind products have reached high quality.

Two important changes affect the speed bias plot: the first is on June 3rd, 1996 and it is due to the switch from ERS-1 to ERS-2 data assimilation in the meteorological model. The second change, which occurred at the beginning of September 1997, is due to the new monitoring and assimilation scheme in ECMWF algorithms (4D-Var).

Since 19th April 1999 two set of meteo-table (meteorological forecast centred at 00:00 and 12:00 of each day) are used in the ground processing. With this new strategy the data are processed using the 18 and 24 hours meteorological forecast instead of the 18, 24, 30 36 hours forecast. The data processed with the 18-24 hours tables instead of 30-36 hours tables have an increase in the number of ambiguity removed nodes but no important improvements are shown, on average, in the daily statistics.

Since 25th August 1999 a new LRDPF software (version 8500) is operative in the ground stations. With this upgrade the LRDPF is year 2000 compatible; no changes were introduced in the scatterometer data processing.

For cycle 48 the PCS quality control has reported stable results apart from days 17th and 18th November 1999 when the ERS-2 payloads were switched off to face out the Leonide meteo shower (no data were acquired).

The ECMWF reports for the cycle 48 an average wind speed bias of -0.82 m/s (UWI-FG) and -0.58 m/s (FG-4D_Var). The wind speed standard deviation is, on average, 1.5 m/s for FG and 1.6 m/s for the 4D_Var analysis.The wind speed biases are slightly larger than in the previous cycle, and are quite likely due to seasonal variations.

The direction standard deviations are ranging between 30 and 65 degrees (UWI-FG) and between 15 and 30 degrees (FG-4D_Var). The directional bias is close to zero for both UWI and 4D_Var analysis. The direction standard deviations are similar to the ones in the previous report period.

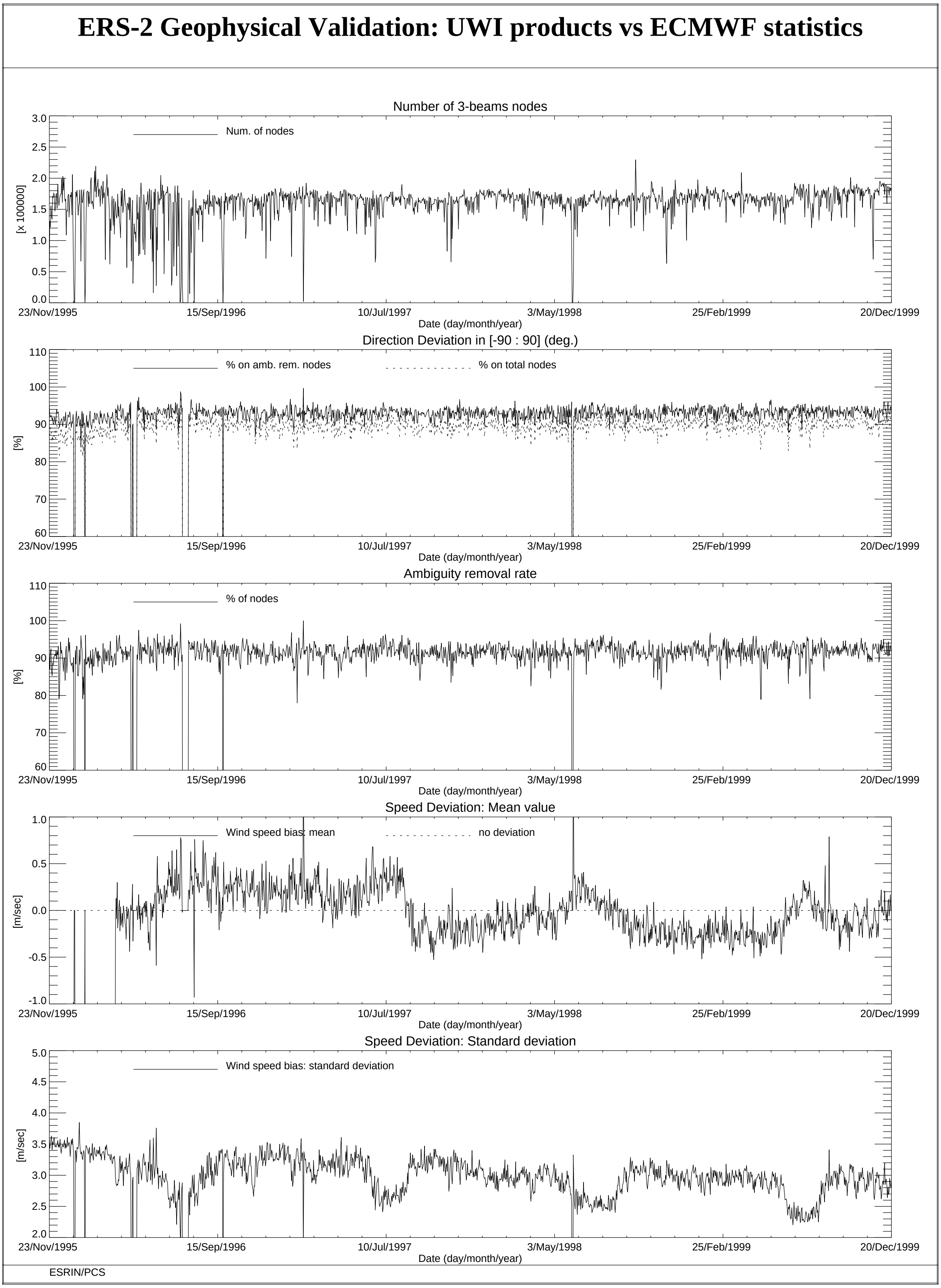

FIGURE 25. ERS-2 Scatterometer: wind products performance since the beginning of the mission.